Eur. Phys. J. C (2023) 83:86
https://doi.org/10.1140/epjc/s10052-023-11219-1

THE EUROPEAN PHYSICAL JOURNAL C

Regular Article - Theoretical Physics

Patterns of gauge symmetry in the background field method

A. C. Aguilar[1,a], **M. N. Ferreira**[2], **D. Ibañez**[3], **B. M. Oliveira**[1], **J. Papavassiliou**[2]

[1] Institute of Physics "Gleb Wataghin", University of Campinas-UNICAMP, Campinas, São Paulo 13083-859, Brazil
[2] Department of Theoretical Physics and IFIC, University of Valencia and CSIC, 46100 Valencia, Spain
[3] University Centre EDEM, Muelle de la Aduana, La Marina de Valencia, 46024 Valencia, Spain

Received: 1 December 2022 / Accepted: 8 January 2023 / Published online: 28 January 2023

Abstract The correlation functions of Yang–Mills theories formulated in the background field method satisfy linear Slavnov–Taylor identities, which are naive generalizations of simple tree level relations, with no deformations originating from the ghost-sector of the theory. In recent years, a stronger version of these identities has been found to hold at the level of the background gluon self-energy, whose transversality is enforced separately for each special block of diagrams contributing to the gluon Schwinger–Dyson equation. In the present work we demonstrate by means of explicit calculations that the same distinct realization of the Slavnov–Taylor identity persists in the case of the background three-gluon vertex. The analysis is carried out at the level of the exact Schwinger–Dyson equation for this vertex, with no truncations or simplifying assumptions. The demonstration entails the contraction of individual vertex diagrams by the relevant momentum, which activates Slavnov–Taylor identities of vertices and multi-particle kernels nested inside these graphs; the final result emerges by virtue of a multitude of extensive cancellations, without the need of performing explicit integrations. In addition, we point out that background Ward identities amount to replacing derivatives of propagators by zero-momentum background-gluon insertions, in exact analogy to standard properties of Abelian gauge theories. Finally, certain potential applications of these results are briefly discussed.

1 Introduction

In recent years, the systematic exploration of Green's (correlation) functions has afforded important insights on the nonperturbative properties of non-Abelian gauge theories, such as pure Yang–Mills theories and Quantum Chromodynamics [1–12]. This ongoing scrutiny relies on continuum studies based on nonperturbative functional methods [7,13–39] carried out almost exclusively in the linear covariant (R_ξ) gauges, where the Landau gauge is the preferred choice, and on lattice simulations performed in the same gauge [40–55]. However, the background field method (BFM) [56–65] has also been employed in several occasions, furnishing useful vantage points, and exposing key properties of the theory that are normally distorted by standard quantization procedures [8,12,66,67].

The BFM is a powerful framework that enables the implementation of the gauge-fixing procedure necessary for quantizing gauge theories without losing explicit gauge invariance, in contradistinction to the conventional quantization schemes [56–65]. The starting point of the BFM is the splitting of the gauge field A^a_μ appearing in the classical action of the theory according to $A^a_\mu = B^a_\mu + Q^a_\mu$, where B^a_μ and Q^a_μ are the background and quantum (fluctuating) fields, respectively. The quantum field is the variable of integration in the generating functional $Z(J)$, and external sources are coupled only to it, as $J \cdot Q$. The background field does not enter in loops; it couples externally to Feynman diagrams, connecting them with the asymptotic states to form S-matrix elements. Then, by virtue of a special gauge-fixing condition, the resulting action (with the corresponding ghost terms included) is no longer invariant under transformations of the quantum field, but retains its invariance intact with respect to the background field [5,63].

A key consequence of the background gauge invariance of the action is that Green's functions involving the B^a_μ field satisfy ghost-free Slavnov–Taylor identities (STIs), akin to the Takahashi identity known from QED: the STIs are straightforward generalization of tree level relations, receiving no ghost-related contributions after the inclusion of quantum corrections. Instead, in the standard STIs [68,69] of the R_ξ gauges [70], starting already at one-loop, the ghost sector modifies these tree level relations non-trivially. To fix the

[a] e-mail: aguilar@ifi.unicamp.br (corresponding author)

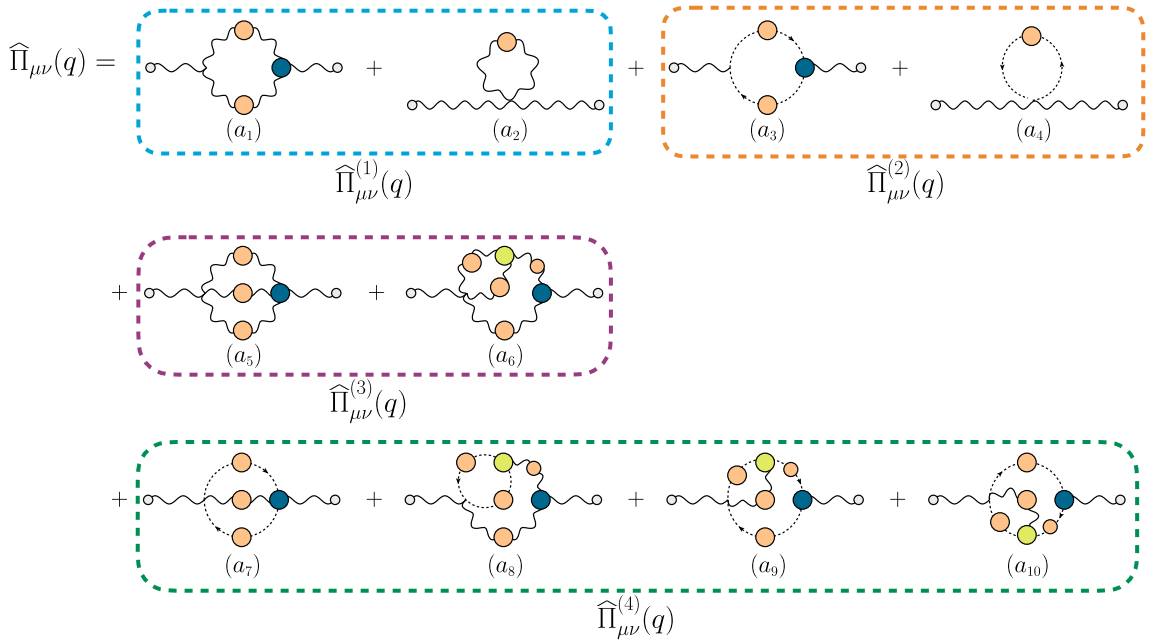

Fig. 1 Diagrammatic representation of the self-energy $\widehat{\Pi}_{\mu\nu}(q)$. The small gray circles at the end of gluon legs indicate a background field. The orange and green circles represent conventional fully dressed propagators and vertices, respectively, while the blue circles represent fully dressed vertices with one background gluon

ideas with a simple example, the quark-gluon vertex with either a B or a Q gluon satisfies at tree level the simple identity (suppressing color) $q^\mu \gamma_\mu = \not{q} = (-\not{p} - m) - (\not{r} - m) = S_0^{-1}(-\not{p}) - S_0^{-1}(\not{r})$, where S_0 is the tree level version of the quark propagator S. In the case of a B gluon, the all-order STI is obtained from the above tree level identity by simply substituting $S_0 \to S$, namely $q^\mu \widehat{\Gamma}_\mu(q, r, p) = S^{-1}(-\not{p}) - S^{-1}(\not{r})$. Instead, in the case of a Q gluon (R_ξ gauges), the STI gets modified by quantum corrections [68,69], which induce a dependence on the ghost dressing function and the quark-ghost kernel [71–74].

As was pointed in earlier studies, the STI satisfied by the background-gluon self-energy, $\widehat{\Pi}_{\mu\nu}(q)$, namely the standard transversality condition $q^\mu \widehat{\Pi}_{\mu\nu}(q) = 0$, is implemented in a very special way, which has been denominated "block-wise" [8,66,67]. Specifically, the diagrammatic representation of the SDE governing $\widehat{\Pi}_{\mu\nu}(q)$ is composed by four distinct blocks, namely one- and two-loop diagrams containing only gluons, and one- and two-loop diagrams containing ghost fields, as shown in Fig. 1. The block-wise realization of the STI in this case is the simple statement that the transversality of $\widehat{\Pi}_{\mu\nu}(q)$ is enforced independently for each of the four blocks. This is in sharp contrast to what happens in the R_ξ gauges, where, already at the one-loop perturbative level, it is only the sum of gluon and ghost diagrams that is transverse [75,76]. The proof of this property is particularly simple; it proceeds by contracting the various diagrams by q^μ from the side of the fully dressed vertices, thus triggering the corresponding naive STIs of the BFM. It is important to emphasize that the proof holds for any value of the gauge-fixing parameter ξ_Q used to define the propagators of the Q-type gluons entering in the various loops.

The basic question that arises naturally in this context is whether the special block-wise realization of the STI described above is particular to the two-point function, or if it is a common feature of all Green's functions containing only B gluons. In the present work we take a first step in the exploration of this issue, and demonstrate that the same pattern persists in the STI of the BFM vertex with three incoming background gluons, to be denoted by $\widehat{\Gamma}_{\alpha\mu\nu}(q, r, p)$. This Abelian STI relates the contraction $q^\mu \widehat{\Gamma}_{\alpha\mu\nu}(q, r, p)$ to the difference $\widehat{\Pi}_{\mu\nu}(r) - \widehat{\Pi}_{\mu\nu}(p)$ [5,66,77]. It turns out that the diagrams comprising the SDE of $\widehat{\Gamma}_{\alpha\mu\nu}(q, r, p)$ may also be classified into four subsets in a way completely analogous to the case of $\widehat{\Pi}_{\mu\nu}(q)$. Then, the contraction of each subset by q^μ generates the difference of the *corresponding* subsets of $\widehat{\Pi}_{\mu\nu}$, confirming the block-wise realization of this STI. We emphasize that, as in the case of the gluon self-energy, this property is completely ξ_Q-independent.

An additional noteworthy aspect of the BFM Green's functions is the Ward identities (WIs) they satisfy, namely the relations that emerge when the momentum that triggers the STIs is taken to vanish. For example, in the case of the $\widehat{\Gamma}_\mu(q, r, p)$ mentioned above, a Taylor expansion of the STI around $q = 0$ and subsequent matching of terms linear in q yields the relation $\widehat{\Gamma}_\mu(0, -p, p) = \partial S^{-1}(\not{p})/\partial p^\mu$, which

is the precise equivalent of the text-book WI known from QED, relating the photon–electron vertex with the electron propagator [75,76]. In fact, exactly as happens in QED, this WI admits a simple diagrammatic interpretation: the derivative of the inverse quark propagator may be depicted as the insertion of a background gluon carrying zero momentum. These observations may be straightforwardly extended to the case of the three-gluon vertex $\widehat{\Gamma}_{\alpha\mu\nu}(q,r,p)$, allowing for a completely analogous pictorial representation of the corresponding WI. In fact, the block-wise realization of the STI leads to a corresponding pattern for the WIs that emerges from it: the derivative acting on *any* of the blocks of $\widehat{\Pi}_{\mu\nu}(q)$ is identical to the diagrams comprising the associated block of $\widehat{\Gamma}_{\alpha\mu\nu}(q,r,p)$, when the corresponding momentum is set to zero. To the best of our knowledge, the notions described above appear for the first time in the literature.

The article is organized as follows. In Sect. 2 we review certain pivotal properties of the BFM, and explain the notion of the block-wise transversality at the level of the SDE that governs the background gluon propagator. Section 3 contains the main result of this work, namely the demonstration of the block-wise realization of the STI for the case of the background three-gluon vertex. Then, in Sect. 4 we focus on the WIs of the BFM, their graphical representation in terms of zero-momentum gluon insertions, and demonstrate the block-wise realization of the three-gluon WI, for the operationally simplest subset of graphs. In Sect. 5 we summarize our findings and discuss future directions. Finally, in four Appendices we present complementary material that facilitates the perusal of the article.

2 General theoretical framework

In this section we highlight some of the significant features of the BFM formalism that are relevant for the demonstrations that follow; for further details the reader is referred to the extensive literature on the subject, see, e.g., [5,61,65].

(i) The initial decomposition of the gauge field into B^a_μ and Q^a_μ components increases considerably the number of Green's functions that can be defined, which may be classified into three broad subsets: those with B^a_μ fields only, those with Q^a_μ fields only (corresponding to the standard Green's functions of the R_ξ gauges), and mixed ones, with both B^a_μ and Q^a_μ fields. We will occasionally denote Green's functions according to the type of incoming fields, such as "BB" for the case of the propagator connecting two background fields, or "BBB" for the case of the three-gluon vertex connecting three such fields.

(ii) The gluon propagator QQ that enters in the quantum loops will be denoted by $\Delta^{ab}_{\mu\nu}(q) = -i\delta^{ab}\Delta_{\mu\nu}(q)$, with

$$\Delta_{\mu\nu}(q) = P_{\mu\nu}(q)\Delta(q) + \xi_Q \frac{q_\mu q_\nu}{q^4},$$
$$P_{\mu\nu}(q) = g_{\mu\nu} - \frac{q_\mu q_\nu}{q^2}, \tag{2.1}$$

whose inverse is

$$\Delta^\nu_\mu(q)\Delta^{-1}_{\nu\rho}(q) = g_{\mu\rho};$$
$$\Delta^{-1}_{\nu\rho}(q) = \Delta^{-1}(q)P_{\nu\rho}(q) + \xi_Q^{-1} q_\nu q_\rho. \tag{2.2}$$

The scalar function $\Delta(q)$ is related to the gluon self-energy $\Pi_{\mu\nu}(q) = P_{\mu\nu}(q)\Pi(q)$ through $\Delta^{-1}(q) = q^2 + i\Pi(q)$, and ξ_Q is the quantum gauge-fixing parameter. Note that ξ_Q enters also in the tree level expressions of the vertices BQQ and BBQQ, given in Table 1.

(iii) In what follows we will use extensively a number of three- and four-particle vertices, which we list here. In particular, the relevant three-particle vertices are

$$\Gamma_{\bar{c}^m c^n Q^a_\mu}(r,p,q) = -gf^{mna}\Gamma_\mu(r,p,q),$$
$$\Gamma_{Q^a_\alpha Q^b_\mu Q^c_\nu}(q,r,p) = gf^{abc}\Gamma_{\alpha\mu\nu}(q,r,p),$$
$$\Gamma_{\bar{c}^m c^n B^a_\mu}(r,p,q) = -gf^{mna}\widetilde{\Gamma}_\mu(r,p,q),$$
$$\Gamma_{B^a_\alpha Q^b_\mu Q^c_\nu}(q,r,p) = gf^{abc}\widetilde{\Gamma}_{\alpha\mu\nu}(q,r,p), \tag{2.3}$$

while the four-particle vertices are

$$\Gamma_{B^a_\mu B^b_\nu \bar{c}^m c^n}(q,r,p,t) = -ig^2\widehat{\Gamma}^{abmn}_{\mu\nu}(q,r,p,t),$$
$$\Gamma_{B^a_\alpha Q^b_\beta Q^c_\mu Q^d_\nu}(q,r,p,t) = -ig^2\widetilde{\Gamma}^{abcd}_{\alpha\beta\mu\nu}(q,r,p,t),$$
$$\Gamma_{B^a_\mu Q^b_\nu \bar{c}^m c^n}(q,r,p,t) = -ig^2\widetilde{\Gamma}^{abmn}_{\mu\nu}(q,r,p,t),$$
$$\Gamma_{B^a_\alpha B^b_\beta Q^b_\mu Q^c_\nu}(q,r,p,t) = -ig^2\widehat{\Gamma}^{abcd}_{\alpha\beta\mu\nu}(q,r,p,t), \tag{2.4}$$

where g denotes the gauge coupling constant, and f^{abc} are the SU(3) structure constants.

(iv) A central quantity in our analysis is the background self-energy, $\widehat{\Pi}_{\mu\nu}(q)$, related to the inverse background gluon propagator $\widehat{\Delta}^{-1}_{\mu\nu}(q)$ by[1]

$$\widehat{\Delta}^{-1}_{\mu\nu}(q) = q^2 P_{\mu\nu}(q) + i\widehat{\Pi}_{\mu\nu}(q). \tag{2.5}$$

The gauge symmetry enforces the fundamental STI

$$q^\mu \widehat{\Pi}_{\mu\nu}(q) = 0, \tag{2.6}$$

from which follows that $\widehat{\Pi}_{\mu\nu}(q) = P_{\mu\nu}(q)\widehat{\Pi}(q)$, where $\widehat{\Pi}(q)$ is a scalar function. Thus, Eq. (2.5) may be cast in

[1] The definition of the BB propagator $\widehat{\Delta}_{\mu\nu}(q)$ requires the addition to the action of a supplementary gauge-fixing term, which introduces the "classical" gauge-fixing parameter, ξ_C [5,61,65]. Note that this step is necessary only when connecting the background gluon to external states in order to construct S-matrix elements, and will be omitted here.

the form

$$\widehat{\Delta}^{-1}_{\mu\nu}(q) = P_{\mu\nu}(q)\left[q^2 + i\,\widehat{\Pi}(q)\right]. \tag{2.7}$$

The SDE that defines $\widehat{\Pi}_{\mu\nu}(q)$ is diagrammatically represented in Fig. 1. Note the separation of the *dressed* Feynman diagrams into the following four distinct groups:

(1) One-loop gluonic graphs, enclosed in the blue box; their total contribution is denoted by $\widehat{\Pi}^{(1)}_{\mu\nu}(q)$.
(2) One-loop ghost graphs, enclosed in the orange box; their total contribution is denoted by $\widehat{\Pi}^{(2)}_{\mu\nu}(q)$.
(3) Two-loop gluonic graphs, enclosed in the purple box; their total contribution is denoted by $\widehat{\Pi}^{(3)}_{\mu\nu}(q)$.
(4) Two-loop ghost graphs, enclosed in the green box; their total contribution is denoted by $\widehat{\Pi}^{(4)}_{\mu\nu}(q)$.

One of the most exceptional properties of $\widehat{\Pi}_{\mu\nu}(q)$ is its block-wise transversality [66,78,79]. Specifically, the fundamental relation given in Eq. (2.6) is realized in a very special way: each of the four subsets of diagrams in Fig. 1 is individually transverse, i.e.,

$$q^\mu\,\widehat{\Pi}^{(i)}_{\mu\nu}(q) = 0, \quad i = 1, 2, 3, 4. \tag{2.8}$$

This particular result is a direct consequence of the Abelian STIs satisfied by the fully dressed vertices entering in the diagrams comprising the $\widehat{\Pi}^{(i)}_{\mu\nu}(q)$ [66,78,79], namely BQQ, B$\bar{\text{c}}$c, BQQQ and BQ$\bar{\text{c}}$c, reported in Table 2 of the Appendix C.

(v) In order to elucidate with a simple example how this special transversality is enforced at the diagrammatic level, we consider the case of $\widehat{\Pi}^{(2)}_{\mu\nu}(q)$, whose diagrams are enclosed by the orange box of Fig. 1.

The diagrams (a_3) and (a_4) are given by

$$(a_3)_{\mu\nu}(q) = \lambda \int_k (2k-q)_\mu D(k-q) D(k) \widetilde{\Gamma}_\nu(q-k, k, -q), \tag{2.9}$$

$$(a_4)_{\mu\nu}(q) = 2\lambda\, g_{\mu\nu} \int_k D(k), \tag{2.10}$$

where we have used the Feynman rules given in Eq. (B2) and Eq. (B6) of the Appendix B, and factored out the trivial color structure δ^{ab} from both expressions. In addition, we have defined

$$\lambda := g^2 C_{\rm A}, \tag{2.11}$$

where $C_{\rm A}$ is the Casimir eigenvalue of the adjoint representation [N for SU(N)]. Furthermore, we have introduced

$$\int_k := \frac{1}{(2\pi)^4} \int_{-\infty}^{+\infty} {\rm d}^4 k, \tag{2.12}$$

where the use of a symmetry-preserving regularization scheme is implicitly assumed.

We next contract graph $(a_3)_{\mu\nu}(q)$ by q^ν, thus triggering the STI satisfied by $\widetilde{\Gamma}_\nu(q-k, k, -q)$, given in Eq. (C2), to obtain

$$\begin{aligned} q^\nu (a_3)_{\mu\nu}(q) &= \lambda \int_k (2k-q)_\mu D(k-q) D(k) \\ &\quad \times \left[D^{-1}(k-q) - D^{-1}(k)\right] \\ &= \lambda \int_k (2k-q)_\mu \left[D(k) - D(k-q)\right] \\ &= -2\lambda\, q_\mu \int_k D(k), \end{aligned} \tag{2.13}$$

which is exactly the negative of the contraction $q^\nu (a_4)_{\mu\nu}(q)$. Hence,

$$q^\nu \left[(a_3)_{\mu\nu}(q) + (a_4)_{\mu\nu}(q)\right] = q^\nu \widehat{\Pi}^{(2)}_{\mu\nu}(q) = 0. \tag{2.14}$$

We emphasize that the above strategy of contracting directly individual diagrams and triggering the corresponding STIs will be followed unaltered in the more complicated case of the three-gluon vertex treated in the next section. Note finally that the entire demonstration leading to Eq. (2.8) is carried out for a general value of the gauge-fixing parameter ξ_Q [66,78,79].

3 Block-wise STI of the three-gluon vertex

In this section we demonstrate the block-wise realization of the STI satisfied by the BBB three-gluon vertex.

3.1 General considerations

(i) The one-particle irreducible three-gluon vertex, $\widehat{\mathbf{\Gamma}}^{abc}_{\alpha\mu\nu}(q, r, p)$, is defined from the vacuum expectation value of the time ordered product of three background gluons (in momentum space), as

$$\begin{aligned} &\langle 0|\, T\left[B^a_{\alpha'}(q)\, B^b_{\mu'}(r)\, B^c_{\nu'}(p)\right]|0\rangle \\ &\quad = g\, \widehat{\mathbf{\Gamma}}^{abc}_{\alpha\mu\nu}(q, r, p) \widehat{\Delta}^\alpha_{\alpha'}(q) \widehat{\Delta}^\mu_{\mu'}(r) \widehat{\Delta}^\nu_{\nu'}(p). \end{aligned} \tag{3.1}$$

The three-gluon vertex $\widehat{\mathbf{\Gamma}}^{abc}_{\alpha\mu\nu}(q, r, p)$ is naturally cast in the form

$$\widehat{\mathbf{\Gamma}}^{abc}_{\alpha\mu\nu}(q, r, p) = \widehat{\Gamma}^{(0)abc}_{\alpha\mu\nu}(q, r, p) + \widehat{\Gamma}^{abc}_{\alpha\mu\nu}(q, r, p), \tag{3.2}$$

where the tree level component $\widehat{\Gamma}^{(0)abc}_{\alpha\mu\nu}(q, r, p) = f^{abc} \widehat{\Gamma}^{(0)}_{\alpha\mu\nu}(q, r, p)$ coincides with that of the conventional three-gluon vertex (QQQ), i.e.,

$$\widehat{\Gamma}^{(0)}_{\alpha\mu\nu}(q, r, p) = \Gamma^{(0)}_{\alpha\mu\nu}(q, r, p) = (q-r)_\nu g_{\alpha\mu}$$

$$+(r-p)_\alpha g_{\mu\nu}+(p-q)_\mu g_{\alpha\nu}, \tag{3.3}$$

while $\widehat{\Gamma}^{abc}_{\alpha\mu\nu}(q,r,p)$ captures all quantum corrections, both perturbative and nonperturbative.

(ii) The SDE that defines $\widehat{\mathbf{\Gamma}}^{abc}_{\alpha\mu\nu}(q,r,p)$ is shown diagrammatically in Fig. 2, written with respect to the gluon that carries momentum q; therefore, the corresponding vertices to which this leg is attached are kept at tree level. The corresponding Feynman diagrams have been classified in four blocks, applying the exact same criterion as in the case of $\widehat{\Pi}_{\mu\nu}(q)$, and employing the same color code for the individual boxes as in Fig. 1. Thus,

$$\widehat{\Gamma}^{abc}_{\alpha\mu\nu}(q,r,p)=\sum_{i=1}^{4}\widehat{\Gamma}^{(i)abc}_{\alpha\mu\nu}(q,r,p), \tag{3.4}$$

where, as shown in Fig. 2, the four blocks are comprised by the diagrams (suppressing indices)

$$\begin{aligned}&\widehat{\Gamma}^{(1)}=(b_1)+(b_2)+(b_3),\quad \widehat{\Gamma}^{(2)}=(c_1)+(c_2)+(c_3),\\ &\widehat{\Gamma}^{(3)}=(d),\quad \widehat{\Gamma}^{(4)}=(e).\end{aligned} \tag{3.5}$$

(iii) It is well-known that $\widehat{\mathbf{\Gamma}}^{abc}_{\alpha\mu\nu}(q,r,p)$ satisfies the Abelian STI [5,66,77]

$$p^\nu\widehat{\mathbf{\Gamma}}^{abc}_{\alpha\mu\nu}(q,r,p)=f^{cae}\left[\widehat{\Delta}^{be}_{\alpha\mu}(r)\right]^{-1}-f^{bce}\left[\widehat{\Delta}^{ae}_{\alpha\mu}(q)\right]^{-1}, \tag{3.6}$$

and cyclic permutations thereof. The STI of Eq. (3.6) may be obtained by means of formal manipulations of the BFM generating functional, or simply from the STI of the conventional QQQ vertex [71,80,81], by setting all ghost-related contributions to their tree level values.

From Eq. (3.3) it is elementary to show that

$$p^\nu\widehat{\Gamma}^{(0)}_{\alpha\mu\nu}(q,r,p)=r^2P_{\alpha\mu}(r)-q^2P_{\alpha\mu}(q). \tag{3.7}$$

Then, from Eqs. (2.5), (3.2) and (3.6) follows that

$$p^\nu\widehat{\Gamma}^{abc}_{\alpha\mu\nu}(q,r,p)=if^{cae}\widehat{\Pi}^{be}_{\alpha\mu}(r)-if^{bce}\widehat{\Pi}^{ae}_{\alpha\mu}(q). \tag{3.8}$$

(iv) The central observation of the present study is that, as happens in the case of Eq. (2.6), the STI in Eq. (3.8) admits a block-wise realization. Specifically, as we will demonstrate in this section,

$$\begin{aligned}&p^\nu\widehat{\Gamma}^{(i)abc}_{\alpha\mu\nu}(q,r,p)=if^{cae}\widehat{\Pi}^{(i)be}_{\alpha\mu}(r)-if^{bce}\widehat{\Pi}^{(i)ae}_{\alpha\mu}(q),\\ &i=1,2,3,4.\end{aligned} \tag{3.9}$$

In diagrammatic terms, Eq. (3.9) states that the contraction by p^ν of the diagrams within a given block (color) in Fig. 2 generates the difference between diagrams within the corresponding block (color) of Fig. 1. In fact, the validity of Eq. (3.9) will be demonstrated by acting with p^ν on vertex diagrams, and exploiting the STIs triggered by this contraction in order to cast the result in the form of self-energy contributions.

(v) Note that the diagrams shown in Fig. 2 have a factor g removed from them, which cancels against the g appearing in the definition of the three-gluon vertex in Eq. (3.1). In addition a factor of i will be factored out, which will cancel against the explicit i appearing on the r.h.s. of Eq. (3.9). Thus, on the r.h.s. of all intermediate formulas will appear directly the self-energy diagrams (a_i) of Fig. 1. Furthermore, with the exception of Sect. 4, we will suppress the argument (q,r,p) in all vertex graphs.

(vi) We introduce the definitions

$$h_1^{abmn}=f^{abe}f^{mne},\quad h_2^{abcde}=f^{abm}f^{cmn}f^{dne}. \tag{3.10}$$

Note that $h_1^{abmn}=h_1^{banm}$ and $h_2^{abcde}=h_2^{baced}$.

(vii) We introduce the short-hand notation

$$\begin{aligned}R^{\alpha\beta}_\mu(r,p)&\equiv\Delta^{\alpha\sigma}(r)\Delta^{\beta\rho}(p)\Gamma_{\mu\sigma\rho}(-r-p,r,p),\\ R_\mu(r,p)&\equiv D(r)D(p)\Gamma_\mu(r,p,-r-p),\\ \widetilde{R}^{\alpha\beta}_\mu(r,p)&\equiv\Delta^{\alpha\sigma}(r)\Delta^{\beta\rho}(p)\widetilde{\Gamma}_{\mu\sigma\rho}(-r-p,r,p),\\ \widetilde{R}_\mu(r,p)&\equiv D(r)D(p)\widetilde{\Gamma}_\mu(r,p,-r-p).\end{aligned} \tag{3.11}$$

The special relations

$$\int_k\widetilde{R}^{\sigma\beta}_\mu(k,r-k)=\int_k\widetilde{R}_\mu(k,r-k)=0, \tag{3.12}$$

will be employed in the analysis that follows. Their validity may be established by appealing to the Bose symmetry of the BQQ vertex with respect to its two quantum legs or the ghost–antighost symmetry of the B$\bar{c}$c vertex, and the change of integration variable $r-k\to k$. An alternative demonstration proceeds by noting that

$$\int_k\widetilde{R}_\mu(k,r-k)=\frac{r_\mu}{r^2}I(r^2), \tag{3.13}$$

with

$$\begin{aligned}I(r^2)&=\int_k D(k)D(r-k)\,r^\mu\widetilde{\Gamma}_\mu(k,r-k,-r)\\ &=\int_k D(k)D(r-k)\left[D^{-1}(k)-D^{-1}(r-k)\right]\\ &=\int_k\left[D(r-k)-D(k)\right]=0,\end{aligned} \tag{3.14}$$

where the STI of Eq. (C2) was used. The first relation in Eq. (3.12) may be proved in the exact same way, employing the STI of Eq. (C1).

(viii) Lastly, from now on we adopt the convention that 1PI vertices containing at least one background gluon will

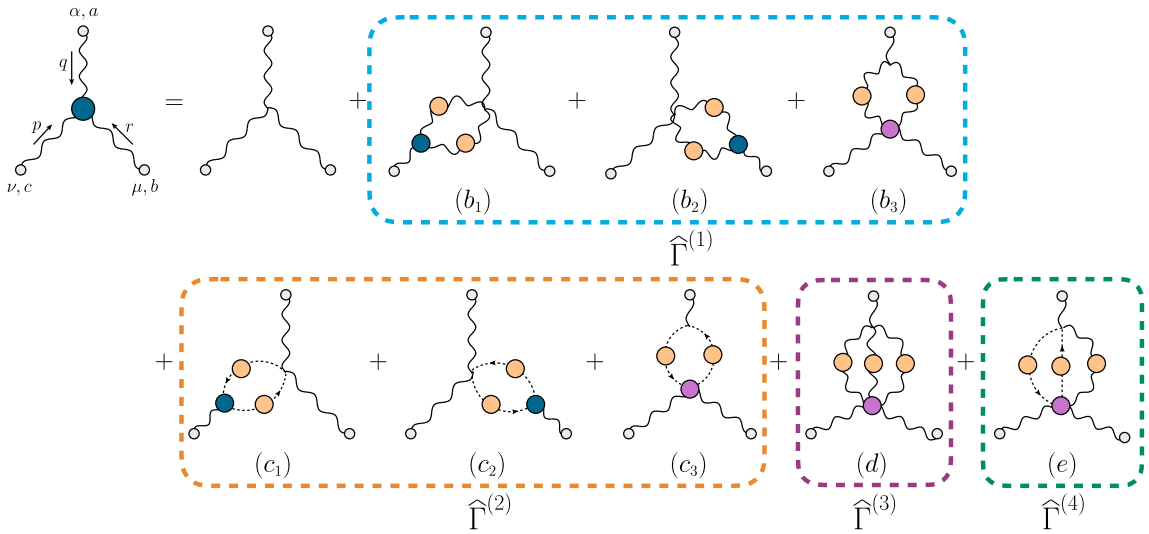

Fig. 2 The block-wise structure of the SDE which describes the three-gluon vertex $\widehat{\mathbf{\Gamma}}^{abc}_{\alpha\mu\nu}(q, r, p)$ (BBB). The blue circles represent full one-particle irreducible vertices, while the purple ones the four- and five-point scattering kernels

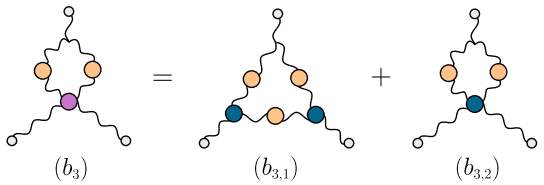

Fig. 3 The two contributions which arise from diagram (b_3) of Fig. 2 after performing the skeleton expansion of the four-gluon scattering kernel (purple blob)

be represented diagrammatically by a blue circle (see, e.g., the BBQQ vertex in diagram $(b_{3,2})$ of Fig. 3).

3.2 One-loop gluonic sector (*first block*)

We begin by considering the one-loop gluonic vertex graphs, namely the set $\{(b_1), (b_2), (b_3)\}$, enclosed in the blue box of Fig. 2.

As a first step, we recognize that, by virtue of Eq. (3.12), diagrams (b_1) and (b_2) vanish,

$$(b_1)^{abc}_{\alpha\mu\nu} = \frac{g^2}{2} f^{ced} \int_k \widehat{\Gamma}^{(0)abde}_{\alpha\mu\beta\sigma} \widetilde{R}^{\sigma\beta}_{\nu}(-k, k-p) = 0,$$
$$(b_2)^{abc}_{\alpha\mu\nu} = \frac{g^2}{2} f^{bed} \int_k \widehat{\Gamma}^{(0)acde}_{\alpha\nu\beta\sigma} \widetilde{R}^{\sigma\beta}_{\mu}(-k, k-r) = 0, \quad (3.15)$$

since $\widehat{\Gamma}^{(0)abde}_{\alpha\mu\beta\sigma}$ is momentum-independent, and may be pulled out of the integral sign.

Diagram (b_3) has two contributions,

$$(b_3)^{abc}_{\alpha\mu\nu} = (b_{3,1})^{abc}_{\alpha\mu\nu} + (b_{3,2})^{abc}_{\alpha\mu\nu}, \quad (3.16)$$

given in Fig. 3, with

$$(b_{3,1})^{abc}_{\alpha\mu\nu} = -\frac{\lambda}{2} f^{abc} \int_k \widetilde{\Gamma}^{(0)}_{\alpha\beta\sigma}(q, k-q, -k) \Delta^{\rho\sigma}(k) \widetilde{R}^{\lambda\beta}_{\mu} \times (k+p, q-k) \widetilde{\Gamma}_{\nu\rho\lambda}(p, k, -k-p),$$
$$(b_{3,2})^{abc}_{\alpha\mu\nu} = \frac{g^2}{2} f^{ade} \int_k \widetilde{\Gamma}^{(0)}_{\alpha\beta\sigma}(q, k-q, -k) \times \Delta^{\beta\rho}(k-q) \Delta^{\sigma\lambda}(k) \widehat{\Gamma}^{cbde}_{\nu\mu\rho\lambda}(p, r, q-k, k). \quad (3.17)$$

The contraction $p^{\nu}(b_3)^{abc}_{\alpha\mu\nu}$ may be evaluated using the STIs in Eqs. (C1) and (C4) and a moderate amount of algebra, yielding

$$p^{\nu}(b_3)^{abc}_{\alpha\mu\nu} = -\frac{\lambda}{2} f^{abc} \int_k \widetilde{\Gamma}^{(0)}_{\alpha\beta\sigma}(q, k-q, -k) \times \left[\widetilde{R}^{\sigma\beta}_{\mu}(k, q-k) + \widetilde{R}^{\sigma\beta}_{\mu}(-k-p, k-q)\right]. \quad (3.18)$$

The first term in Eq. (3.18) is exactly $-f^{bce}(a_1)^{ae}_{\alpha\mu}(q)$. The second term, after $k \to -k-p$, generates $f^{cae}(a_1)^{be}_{\alpha\mu}(r)$; note, in particular, that

$$\widetilde{\Gamma}^{(0)}_{\alpha\beta\sigma}(q, k-q, -k) \to -\widetilde{\Gamma}^{(0)}_{\alpha\beta\sigma}(r, k-r, -k) + 2p_{\beta} g_{\alpha\sigma} - p_{\alpha} g_{\beta\sigma} - (\xi_Q^{-1} + 1) p_{\sigma} g_{\alpha\beta}, \quad (3.19)$$

where, due to Eq. (3.12), the last three terms give vanishing contributions. Thus, one arrives at

$$p^{\nu}(b_3)^{abc}_{\alpha\mu\nu} = f^{cae}(a_1)^{be}_{\alpha\mu}(r) - f^{bce}(a_1)^{ae}_{\alpha\mu}(q). \quad (3.20)$$

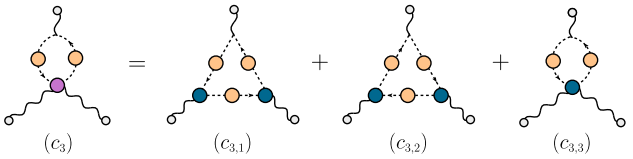

Fig. 4 The three contributions which emerge from the diagram (c_3) shown in the Fig. 2, after implementing the skeleton expansion of the four-point scattering kernel (purple blob) formed by two background gluons with a ghost–antighost pair

At this point, we add and subtract on the r.h.s. of Eq. (3.20) the momentum-independent seagull graph (a_2), to obtain

$$p^{\nu}(b_3)^{abc}_{\alpha\mu\nu} = f^{cae}[(a_1)+(a_2)]^{be}_{\alpha\mu}(r) - f^{bce}[(a_1)+(a_2)]^{ae}_{\alpha\mu}(q), \tag{3.21}$$

which, in view of Eq. (3.15), is precisely Eq. (3.9) for $i=1$.

3.3 One-loop ghost sector (*second block*)

We next focus on the one-loop ghost graphs, forming the set $\{(c_1),(c_2),(c_3)\}$, enclosed in the orange box of Fig. 2. The demonstration that follows is completely analogous to that of the previous subsection.

Due to Eq. (3.12), diagrams (c_1) and (c_2) vanish,

$$(c_1)^{abc}_{\alpha\mu\nu} = g^2 f^{edc}\int_k \widehat{\Gamma}^{(0)abde}_{\alpha\mu}\widetilde{R}_{\nu}(-k,k-p)=0,$$
$$(c_2)^{abc}_{\alpha\mu\nu} = g^2 f^{edb}\int_k \widehat{\Gamma}^{(0)acde}_{\alpha\nu}\widetilde{R}_{\mu}(-k,k-r)=0, \tag{3.22}$$

and we only need to consider the contraction of graph (c_3). This diagram contains three contributions, depicted in Fig. 4,

$$(c_3)^{abc}_{\alpha\mu\nu} = \sum_{j=1}^{3}(c_{3,j})^{abc}_{\alpha\mu\nu}, \tag{3.23}$$

with

$$(c_{3,1})^{abc}_{\alpha\mu\nu} = -\frac{\lambda}{2}f^{abc}\int_k (2k-q)_{\alpha}D(k-q)\widetilde{R}_{\mu}(k,-k-r) \times \widetilde{\Gamma}_{\nu}(k+r,q-k,p),$$
$$(c_{3,2})^{abc}_{\alpha\mu\nu} = -\frac{\lambda}{2}f^{abc}\int_k (2k-q)_{\alpha}D(k-q)\widetilde{R}_{\mu}(-k-r,k) \times \widetilde{\Gamma}_{\nu}(q-k,k+r,p),$$
$$(c_{3,3})^{abc}_{\alpha\mu\nu} = -g^2 f^{eda}\int_k (2k-q)_{\alpha}D(k)D(q-k) \times \widehat{\Gamma}^{bcde}_{\mu\nu}(r,p,q-k,k). \tag{3.24}$$

The contraction of diagram (c_3) by the momentum p^{ν} activates the STIs of Eqs. (C2) and (C6), and one obtains.

$$p^{\nu}(c_3)^{abc}_{\alpha\mu\nu} = -\lambda f^{abc}\int_k (2k-q)_{\alpha} \times\left[\widetilde{R}_{\mu}(k-q,-p-k)+\widetilde{R}_{\mu}(q-k,k)\right]. \tag{3.25}$$

The second term of Eq. (3.25) is simply $-f^{bce}(a_3)^{ae}_{\alpha\mu}(q)$, while the first term, after the shift $k\to -k-p$ and use of Eq. (3.12), furnishes $f^{cae}(a_3)^{be}_{\alpha\mu}(r)$. Thus, we conclude that

$$p^{\nu}(c_3)^{abc}_{\alpha\mu\nu} = f^{cae}(a_3)^{be}_{\alpha\mu}(r) - f^{bce}(a_3)^{ae}_{\alpha\mu}(q), \tag{3.26}$$

which, after adding and subtracting the momentum-independent (a_4), is tantamount to the validity of Eq. (3.9) for $i=2$.

3.4 Two-loop gluonic sector (*third block*)

We turn to the two-loop dressed gluonic contributions, contained within the diagram (d), enclosed by the purple box in Fig. 2. To that end, in Fig. 5 we show the individual diagrams that emerge upon implementing the skeleton expansion of the five-gluon kernel (purple circle) inside (d). Note that all vertices appearing in these graphs are one-particle irreducible.

The diagrams in Fig. 5 are naturally organized into two subsets,

$$(d)^{abc}_{\alpha\mu\nu} = (d_1)^{abc}_{\alpha\mu\nu} + (d_2)^{abc}_{\alpha\mu\nu}, \tag{3.27}$$

with

$$(d_1)^{abc}_{\alpha\mu\nu} = \sum_{j=1}^{2}(d_{1,j})^{abc}_{\alpha\mu\nu}, \quad (d_2)^{abc}_{\alpha\mu\nu} = \sum_{j=1}^{5}(d_{2,j})^{abc}_{\alpha\mu\nu}, \tag{3.28}$$

where

$$(d_{1,1})^{abc}_{\alpha\mu\nu} = \frac{ig^4}{2}f^{cen}\int_k\int_l \widetilde{\Gamma}^{(0)adme}_{\alpha\beta\sigma\rho}\Delta^{\beta\tau}(k)\Delta^{\sigma\eta}(s) \times \widetilde{R}^{\rho\lambda}_{\nu}(l,-p-l)\widetilde{\Gamma}^{bnmd}_{\mu\lambda\eta\tau}(r,l+p,s,k),$$
$$(d_{1,2})^{abc}_{\alpha\mu\nu} = -\frac{ig^4}{6}\int_k\int_l \widetilde{\Gamma}^{(0)adme}_{\alpha\beta\sigma\rho}\Delta^{\beta\tau}(k)\Delta^{\sigma\eta}(s) \times \Delta^{\rho\lambda}(l)\widehat{\Gamma}^{cbemd}_{\nu\mu\lambda\eta\tau}(p,r,l,s,k), \tag{3.29}$$

and

$$(d_{2,1})^{abc}_{\alpha\mu\nu} = \frac{ig^4}{2}f^{ben}\int_k\int_l \widetilde{\Gamma}^{(0)adme}_{\alpha\beta\sigma\rho}\Delta^{\beta\tau}(k)\Delta^{\sigma\eta}(s) \times \widetilde{R}^{\rho\lambda}_{\mu}(l,-r-l)\widetilde{\Gamma}^{cnmd}_{\nu\lambda\eta\tau}(p,l+r,s,k),$$
$$(d_{2,2})^{abc}_{\alpha\mu\nu} = \frac{ig^4}{2}h_2^{dmbec}\int_k\int_l \widetilde{\Gamma}^{(0)adme}_{\alpha\beta\sigma\rho}\Delta^{\rho\lambda}(l)R^{\sigma\beta}_{\tau}(s,k)$$

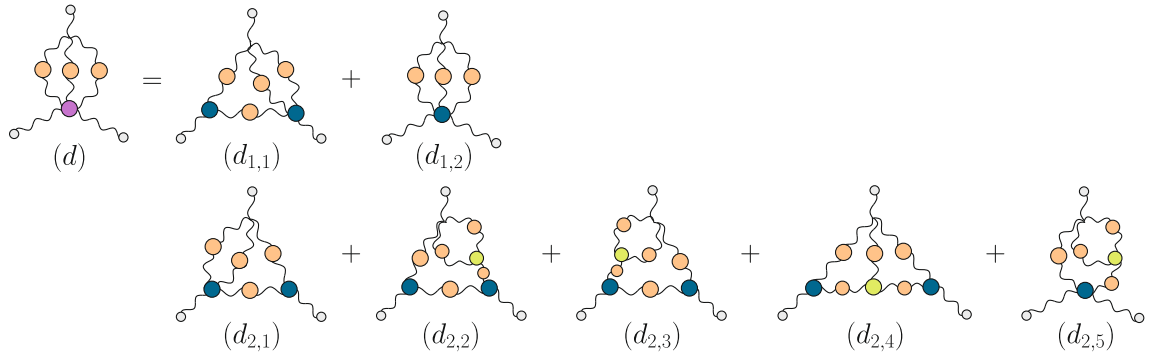

Fig. 5 The seven contributions originating from diagram (d) of the Fig. 2. This group splits into two subsets: the first composed by the diagrams $\{(d_{1,1}), (d_{1,2})\}$ and the second by $\{(d_{2,1}), (d_{2,2}), (d_{2,3}), (d_{2,4}), (d_{2,5})\}$

$$\times\ \widetilde{R}^{\eta\tau}_{\mu}(l+p,q-l)\widetilde{\Gamma}_{\nu\lambda\eta}(p,l,-l-p),$$

$$(d_{2,3})^{abc}_{\alpha\mu\nu} = \frac{ig^4}{2}h_2^{dmceb}\int_k\int_l \widetilde{\Gamma}^{(0)adme}_{\alpha\beta\sigma\rho}\Delta^{\beta\tau}(k)R^{\eta\sigma}_{\tau}(l-q,s) \times\ \widetilde{R}^{\rho\lambda}_{\mu}(l,-r-l)\widetilde{\Gamma}_{\nu\lambda\eta}(p,l+r,q-l),$$

$$(d_{2,4})^{abc}_{\alpha\mu\nu} = ig^4h_2^{cdmbe}\int_k\int_l \widetilde{\Gamma}^{(0)adme}_{\alpha\beta\sigma\rho}\Delta^{\beta\eta}(k)\widetilde{R}^{\rho\tau}_{\mu}(l,-r-l) \times\ R^{\sigma\lambda}_{\tau}(s,k+p)\widetilde{\Gamma}_{\nu\lambda\eta}(p,-k-p,k),$$

$$(d_{2,5})^{abc}_{\alpha\mu\nu} = \frac{ig^4}{2}f^{mdn}\int_k\int_l \widetilde{\Gamma}^{(0)adme}_{\alpha\beta\sigma\rho}\Delta^{\beta\tau}(k)\Delta^{\rho\lambda}(l)R^{\eta\sigma}_{\tau}(l-q,s) \times\ \widehat{\Gamma}^{cben}_{\nu\mu\lambda\eta}(p,r,l,q-l). \tag{3.30}$$

This particular separation is motivated by the observation that the contraction by p^ν of each subset generates a concrete term of the STI, namely

$$p^\nu(d_1)^{abc}_{\alpha\mu\nu} = f^{cae}(a_5)^{be}_{\alpha\mu}(r) - f^{bce}(a_5)^{ae}_{\alpha\mu}(q),$$
$$p^\nu(d_2)^{abc}_{\alpha\mu\nu} = f^{cae}(a_6)^{be}_{\alpha\mu}(r) - f^{bce}(a_6)^{ae}_{\alpha\mu}(q), \tag{3.31}$$

where the self-energy diagrams (a_5) and (a_6) (purple box in Fig. 1) are given by

$$(a_5)^{ab}_{\alpha\mu}(q) = -\frac{ig^4}{6}\int_k\int_l \widetilde{\Gamma}^{(0)adme}_{\alpha\beta\sigma\rho}\Delta^{\beta\tau}(k)\Delta^{\sigma\eta}(s)\Delta^{\rho\lambda}(l) \times\ \widetilde{\Gamma}^{bemd}_{\mu\lambda\eta\tau}(-q,l,s,k) = ig^4h_1^{adme}\int_k\int_l \Delta^{\beta\tau}(k)\Delta^{\eta}_{\beta}(s)\Delta^{\lambda}_{\alpha}(l) \times\ \widetilde{\Gamma}^{bemd}_{\mu\lambda\eta\tau}(-q,l,s,k),$$

$$(a_6)^{ab}_{\alpha\mu}(q) = \frac{ig^4}{2}h_1^{bedm}\int_k\int_l \widetilde{\Gamma}^{(0)adme}_{\alpha\beta\sigma\rho}\widetilde{R}^{\rho\lambda}_{\mu}(l,q-l)R^{\sigma\beta}_{\lambda}(s,k), \tag{3.32}$$

with $s = q-k-l$. In passing from the first to the second expression for (a_5), the explicit form of $\widetilde{\Gamma}^{(0)adme}_{\alpha\beta\sigma\rho}$, given in Eq. (B3), has been used.

The contraction of the momentum p^ν with the above diagrams will activate a series of STIs, which will furnish the desired structures, together with a considerable number of terms that will cancel exactly among each other. In what follows, we briefly outline how this calculation may be best organized.

We begin with the diagrams comprising $(d_1)^{abc}_{\alpha\mu\nu}$. The action of p^ν on $(d_{1,1})^{abc}_{\alpha\mu\nu}$ leads to the contraction $p^\nu\widetilde{R}^{\rho\lambda}_{\nu}(l,-p-l)$, triggering the STI of Eq. (C1), and yielding

$$p^\nu\widetilde{R}^{\rho\lambda}_{\nu}(l,-p-l) = \Delta^{\rho\alpha}(l)\Delta^{\lambda\beta}(l+p)N \times\left[\Delta^{-1}_{\alpha\beta}(l+p) - \Delta^{-1}_{\alpha\beta}(l)\right] = \Delta^{\rho\lambda}(l) - \Delta^{\rho\lambda}(l+p). \tag{3.33}$$

The second term in the above expression will give

$$p^\nu(d_{1,1})^{abc}_{\alpha\mu\nu} = -\frac{ig^4}{2}f^{cen}\int_k\int_l \widetilde{\Gamma}^{(0)adme}_{\alpha\beta\sigma\rho}\Delta^{\beta\tau}(k)\Delta^{\sigma\eta}(s) \times\ \Delta^{\rho\lambda}(l+p)\widetilde{\Gamma}^{bnmd}_{\mu\lambda\eta\tau}(r,l+p,s,k)+\cdots, \tag{3.34}$$

where the ellipsis denotes terms that do not contribute to the r.h.s. of Eq. (3.31). We now change the integration variables as $k\to -k$ and $l\to -l-p$, and exploit Lorentz invariance to replace $\widetilde{\Gamma}^{bnmd}_{\mu\lambda\eta\tau}(r,-l,-t,-k)\to\widetilde{\Gamma}^{bnmd}_{\mu\lambda\eta\tau}(-r,l,t,k)$ and $s\to -t$, where $t = r-k-l$. Then, substituting the Feynman rule of Eq. (B3) and using the Bose symmetry of the vertices, we arrive at

$$p^\nu(d_{1,1})^{abc}_{\alpha\mu\nu} = ig^4f^{cae}h_1^{edmn}\int_k\int_l \Delta^{\beta\tau}(k)\Delta^{\eta}_{\beta}(t)\Delta^{\lambda}_{\alpha}(l) \times\ \widetilde{\Gamma}^{bnmd}_{\mu\lambda\eta\tau}(-r,l,t,k)+\cdots, \tag{3.35}$$

which is precisely $f^{cae}(a_5)^{be}_{\mu\nu}(r)$, in the form given in the second line of Eq. (3.32).

Similarly, the contraction of $(d_{1,2})^{abc}_{\alpha\mu\nu}$ by p^ν activates the STI for the five-point function $\widehat{\Gamma}^{cbemd}_{\nu\mu\lambda\eta\tau}(p,r,l,s,k)$, given in Eq. (C7), namely

$$p^\nu\widehat{\Gamma}^{cbemd}_{\nu\mu\lambda\eta\tau}(p,r,l,s,k) = f^{bcx}\widetilde{\Gamma}^{xemd}_{\mu\lambda\eta\tau}(r+p,l,s,k)$$

$$+ f^{ecx}\widetilde{\Gamma}^{bxmd}_{\mu\lambda\eta\tau}(r, l+p, s, k) + f^{mcx}\widetilde{\Gamma}^{bexd}_{\mu\lambda\eta\tau}(r, p, s+p, k) + f^{dcx}\widetilde{\Gamma}^{bemx}_{\mu\lambda\eta\tau}(r, p, s, k+p). \tag{3.36}$$

Note that only the first term on the r.h.s. of Eq. (3.36) contains the four-point function with a q entry, since $r + p = -q$. Thus, one gets

$$p^{\nu}(d_{1,2})^{abc}_{\alpha\mu\nu} = \frac{ig^4}{6} f^{bcx}\int_k\int_l \widetilde{\Gamma}^{(0)adme}_{\alpha\beta\sigma\rho}\Delta^{\beta\tau}(k)\Delta^{\sigma\eta}(s) \times \Delta^{\rho\lambda}(l)\widetilde{\Gamma}^{xemd}_{\mu\lambda\eta\tau}(-q, l, s, k) + \cdots, \tag{3.37}$$

which is precisely $f^{bce}(a_5)^{ae}(q)$.

After appropriate changes in the integration variables and judicious use of Bose symmetry, one may show that all remaining terms, denoted by the ellipses in Eqs. (3.35) and (3.37), cancel against each other. Thus, one is left with the first equation in Eq. (3.31).

A similar line of reasoning reveals that the term $f^{cae}(a_6)^{be}_{\alpha\mu}(r)$ originates from the contraction of p^{ν} with the diagrams $(d_{2,2})$ and $(d_{2,4})$ of the second group. Specifically, one triggers the STI of Eq. (C1), to obtain

$$p^{\nu}\left[(d_{2,2})+(d_{2,4})\right]^{abc}_{\alpha\mu\nu} = \frac{ig^4}{2}\left[h_2^{dmbec}+2h_2^{cdmbe}\right] \times \int_k\int_l \widetilde{\Gamma}^{(0)adme}_{\alpha\beta\sigma\rho}\widetilde{R}^{\rho\lambda}_{\mu}(l, r-l)R^{\sigma\beta}_{\lambda}(t, k) + \cdots. \tag{3.38}$$

Using the Feynman rule given by Eq. (B3) for the tree level vertex one gets that

$$\frac{ig^4}{2}\left[h_2^{dmbec}+2h_2^{cdmbe}\right]\widetilde{\Gamma}^{(0)adme}_{\alpha\beta\sigma\rho} = \frac{ig^4}{2} f^{cax}h_1^{bedm}\widetilde{\Gamma}^{(0)xdme}_{\alpha\beta\sigma\rho} + \cdots; \tag{3.39}$$

the substitution of the first term into Eq. (3.38) gives precisely $f^{cae}(a_6)^{be}_{\alpha\mu}(r)$, while the ellipsis contains the terms that will cancel.

Finally, the contraction of $(d_{2,5})$ by p^{ν} activates the STI of Eq. (C4), giving

$$p^{\nu}(d_{2,5})^{abc}_{\alpha\mu\nu} = -\frac{ig^4}{2} f^{bcx}h_1^{xedm}\int_k\int_l \widetilde{\Gamma}^{(0)adme}_{\alpha\beta\sigma\rho}\widetilde{R}^{\rho\lambda}_{\mu}(l, q-l) \times R^{\sigma\beta}_{\lambda}(s, k) + \cdots, \tag{3.40}$$

which is exactly $-f^{bce}(a_6)^{ae}_{\alpha\mu}(q)$.

Once again, all the terms inside the ellipses in Eqs. (3.38) and (3.40), cancel exactly against the terms coming from $p^{\nu}\left[(d_{2,1})+(d_{2,3})\right]_{\alpha\mu\nu}$, leading to the second line in Eq. (3.31).

Thus, the above considerations demonstrate the validity of Eq. (3.9) for $i = 3$.

3.5 Two-loop ghost sector (*fourth block*)

Finally, the two-loop dressed ghost graphs, given by the diagram (e), enclosed by the green box in Fig. 2, have twenty two contributions, depicted in Fig. 6, which have been further separated into three subgroups as

$$(e)^{abc}_{\alpha\mu\nu} = \sum_{i=1}^{3}(e_i)^{abc}_{\alpha\mu\nu}, \tag{3.41}$$

with

$$(e_1)^{abc}_{\alpha\mu\nu} = \sum_{j=1}^{4}(e_{1,j})^{abc}_{\alpha\mu\nu}, \quad (e_2)^{abc}_{\alpha\mu\nu} = \sum_{j=1}^{6}(e_{2,j})^{abc}_{\alpha\mu\nu}, \quad (e_3)^{abc}_{\alpha\mu\nu} = \sum_{j=1}^{12}(e_{3,j})^{abc}_{\alpha\mu\nu}, \tag{3.42}$$

such that

$$\begin{aligned} p^{\nu}(e_1)^{abc}_{\alpha\mu\nu} &= f^{cae}(a_7)^{be}_{\alpha\mu}(r) - f^{bce}(a_7)^{ae}_{\alpha\mu}(q), \\ p^{\nu}(e_2)^{abc}_{\alpha\mu\nu} &= f^{cae}(a_8)^{be}_{\alpha\mu}(r) - f^{bce}(a_8)^{ae}_{\alpha\mu}(q), \\ p^{\nu}(e_3)^{abc}_{\alpha\mu\nu} &= f^{cae}\left[(a_9)+(a_{10})\right]^{be}_{\alpha\mu}(r) - f^{bce}\left[(a_9)+(a_{10})\right]^{ae}_{\alpha\mu}(q). \end{aligned} \tag{3.43}$$

The expressions for all the diagrams in Fig. 6, together with the associated self-energy graphs, are given in the Appendix D.

A close inspection of these expressions reveals that

$$\begin{aligned} p^{\nu}(e_{1,4})^{abc}_{\alpha\mu\nu} &= -f^{bce}(a_7)^{ae}_{\alpha\mu}(q)+\cdots, \\ p^{\nu}(e_{3,6})^{abc}_{\alpha\mu\nu} &= -f^{bce}(a_9)^{ae}_{\alpha\mu}(q)+\cdots, \\ p^{\nu}(e_{2,6})^{abc}_{\alpha\mu\nu} &= -f^{bce}(a_8)^{ae}_{\alpha\mu}(q)+\cdots, \\ p^{\nu}(e_{3,12})^{abc}_{\alpha\mu\nu} &= -f^{bce}(a_{10})^{ae}_{\alpha\mu}(q)+\cdots, \end{aligned} \tag{3.44}$$

and

$$\begin{aligned} p^{\nu}\left[(e_{1,1})+(e_{1,2})+(e_{1,3})\right]^{abc}_{\alpha\mu\nu} &= f^{cae}(a_7)^{be}_{\alpha\mu}(r)+\cdots, \\ p^{\nu}\left[(e_{2,2})+(e_{2,4})\right]^{abc}_{\alpha\mu\nu} &= f^{cae}(a_8)^{be}_{\alpha\mu}(r)+\cdots, \\ p^{\nu}\left[(e_{3,3})+(e_{3,4})+(e_{3,9})+(e_{3,10})\right]^{abc}_{\alpha\mu\nu} &= f^{cae}\left[(a_9)+(a_{10})\right]^{be}_{\alpha\mu}(r)+\cdots. \end{aligned} \tag{3.45}$$

It is then a matter of straightforward algebra to demonstrate that all terms contained in the ellipses of Eqs. (3.44)

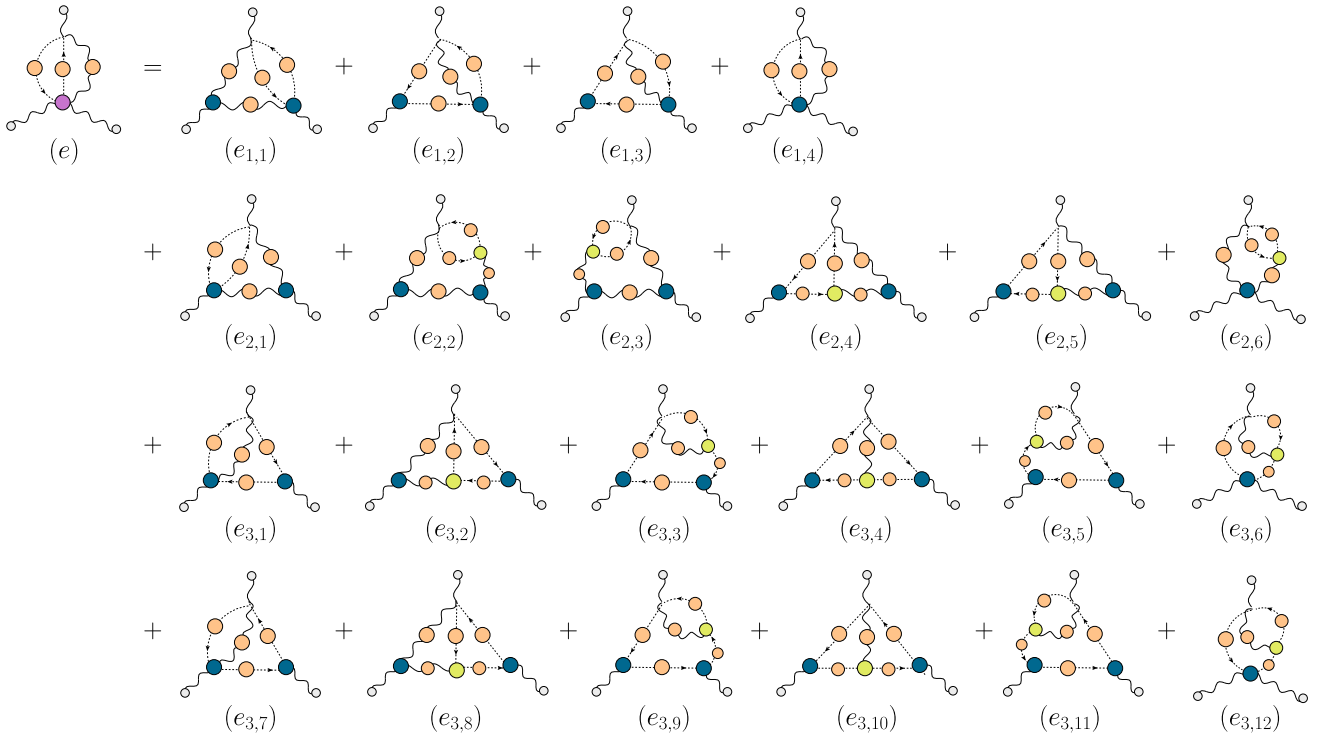

Fig. 6 Contributions from the diagram (e) in Fig. 2 after expanding the five-point kernel represented by the purple blob. This group is organized in the three subsets (e_1), (e_2), and (e_3)

and (3.45) cancel against each other and with the other diagrams, as

$$
\begin{aligned}
&p^\nu[(e_{2,1}) + (e_{2,3}) + (e_{2,5})]^{abc}_{\alpha\mu\nu} + \cdots = 0,\\
&p^\nu[(e_{3,1}) + (e_{3,2}) + (e_{3,3}) + (e_{3,5}) + (e_{3,7}) + (e_{3,8})\\
&\quad + (e_{3,11})]^{abc}_{\alpha\mu\nu} + \cdots = 0,
\end{aligned}
\tag{3.46}
$$

leaving Eq. (3.43) as the final result. Thus, the validity of Eq. (3.9) for $i = 4$ is confirmed.

The final conclusion drawn from the analysis presented in Sects. 3.2, 3.3, 3.4, and 3.5 is that the block-wise realization of the STI announced in Sect. 3.1, holds. Notice, in fact, that the validity of Eq. (3.9) has been demonstrated for an *arbitrary* value of the gauge-fixing parameter ξ_Q.

4 Abelian Ward identities with background gluons

In this section we derive Abelian WIs from the STIs satisfied by the BFM vertices, and apply to them the text-book diagrammatic representation for the WIs known from QED [75]. In addition, we demonstrate the block-wise realization of the WI that connects the vertex $\widehat{\Gamma}_{\alpha\mu\nu}(0, r, -r)$ with the derivative of $\widehat{\Delta}(r)$.

As is well-known in the context of Abelian gauge theories, such as spinor or scalar QED, the implementation of the limit $q \to 0$ of the Takahashi identity gives rise to the corresponding WI. In order to fix the ideas consider the latter theory, describing the interaction of a photon with a complex scalar, where the full photon-scalar vertex $\Gamma_\mu(r, p, q)$ satisfies the Abelian STI (Takahashi identity)

$$
q^\mu \Gamma_\mu(r, p, q) = \mathcal{D}^{-1}(p) - \mathcal{D}^{-1}(r), \tag{4.1}
$$

with $\mathcal{D}(p)$ denoting the fully dressed propagator of the scalar field. Then, the standard WI is determined by expanding both sides of Eq. (4.1) around $q = 0$, and equating the linear terms. Specifically, this procedure yields

$$
\Gamma_\mu(r, -r, 0) = \frac{\partial\, \mathcal{D}^{-1}(r)}{\partial r^\mu}, \tag{4.2}
$$

or, equivalently,

$$
\frac{\partial\, \mathcal{D}(r)}{\partial r^\mu} = -\mathcal{D}(r)\Gamma_\mu(r, -r, 0)\mathcal{D}(r). \tag{4.3}
$$

The version of the WI given in Eq. (4.3) admits the text-book diagrammatic interpretation: the derivative of the propagator $\mathcal{D}(r)$ is equivalent to the insertion of a zero-momentum photon in it [75].

It turns out that the Abelian STIs satisfied by the BFM three-point functions give rise to WIs completely analogous

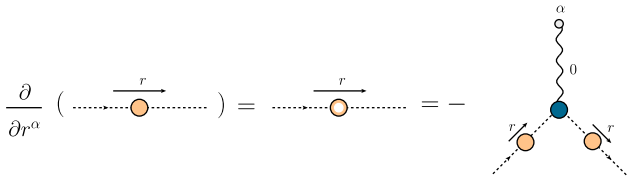

Fig. 7 Diagrammatic representation of the WI for the B$\bar{c}$c vertex, where the derivative of the ghost propagator can be identified as the insertion of a zero-momentum background gluon leg. Here we define the notation of a perforated circle as being the derivative acting on the Green's function

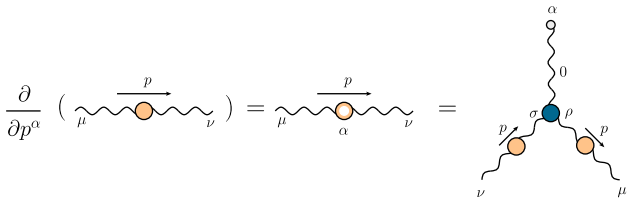

Fig. 8 Diagrammatic representation of the WI for the BQQ vertex, where the derivative of the gluon propagator can be identified as the insertion of a zero-momentum background gluon leg

to that of Eq. (4.3), which admit the same diagrammatic interpretation given above, but now in terms of zero-momentum insertions of a background gluon.

The simplest case is that of the ghost-gluon vertex $\widetilde{\Gamma}_\mu(r,\,p,\,q)$, whose WI is identical to that of Eqs. (4.2) and (4.3), after the replacement $\Gamma_\mu \to \widetilde{\Gamma}_\mu$ and $\mathcal{D} \to D$, i.e.,

$$\begin{aligned}\widetilde{\Gamma}_\mu(r,-r,0) &= \frac{\partial\, D^{-1}(r)}{\partial r^\mu} \Longrightarrow \frac{\partial\, D(r)}{\partial r^\mu} \\ &= -D(r)\widetilde{\Gamma}_\mu(r,-r,0)D(r);\end{aligned} \tag{4.4}$$

the corresponding diagrammatic representation is shown in Fig. 7.

Turning to the case of the BQQ vertex $\widetilde{\Gamma}_{\alpha\mu\nu}(q,r,p)$, it is rather straightforward to deduce from the STI of Eq. (C1) the corresponding WI, namely

$$\begin{aligned}\widetilde{\Gamma}_{\alpha\mu\nu}(0,-p,\,p) &= -\frac{\partial\Delta^{-1}_{\mu\nu}(p)}{\partial p^\alpha} \Longrightarrow \frac{\partial\Delta^{\mu\nu}(p)}{\partial p^\alpha} \\ &= \Delta^{\mu\rho}(p)\,\widetilde{\Gamma}_{\alpha\rho\sigma}(0,-p,\,p)\,\Delta^{\nu\sigma}(p);\end{aligned} \tag{4.5}$$

the last relation is diagrammatically depicted in Fig. 8. Note that the above WI, when applied at tree level, reproduces from Eq. (2.2) the expression for $\widetilde{\Gamma}^{(0)}_{\alpha\mu\nu}(q,r,p)$ given in Eq. (B1), capturing correctly its dependence on the gauge-fixing parameter ξ_Q.

We next focus our attention on the WIs satisfied by BFM vertices with more than three incoming fields. As a concrete example, consider the vertex BB$\bar{c}$c; when contracted with respect to the momentum carried by one of the background gluons, it satisfies the STI given by Eq. (C6). Expanding both sides of Eq. (C6) around $q = 0$, and using the Jacobi identity to eliminate the zeroth order term on the r.h.s., we obtain the WI

$$\begin{aligned}&\widetilde{\Gamma}^{abmn}_{\mu\nu}(0,-p-t,\,p,\,t) \\ &\quad= \left(f^{amx}f^{nbx}\frac{\partial}{\partial p^\mu} + f^{anx}f^{bmx}\frac{\partial}{\partial t^\mu}\right) \\ &\qquad\times \widetilde{\Gamma}_\nu(p,\,t,\,-p-t).\end{aligned} \tag{4.6}$$

Exactly analogous expressions may be deduced for higher point Green's functions; for a formal derivation of the STI satisfied by a general vertex of the form BQ^n, see Appendix A.

Now we want to explore the block-wise realization of the WI of the BBB vertex for the case of the one-loop ghost group, which satisfies the STI of Eq. (3.9) for $i = 2$, or, equivalently, Eq. (3.26). In the soft-gluon limit, we obtain simply

$$\widehat{\Gamma}^{(2)}_{\alpha\mu\nu}(q,-q,0) = \frac{\partial\widehat{\Pi}^{(2)}_{\alpha\mu}(q)}{\partial q^\nu}, \tag{4.7}$$

or, in terms of diagrams

$$(c_3)_{\alpha\mu\nu}(q,-q,0) = \frac{\partial(a_3)_{\alpha\mu}(q)}{\partial q^\nu}. \tag{4.8}$$

In arriving at Eq. (4.8) we have used that (a_4) is q-independent, and that, in the soft-gluon limit, $(c_1) = (c_2) = 0$ (see Sect. 3.3).

To prove Eq. (4.8), we first symmetrize the process of differentiation of $(a_3)_{\alpha\mu}$ by shifting the loop momentum $(k \to u - k$, with $u = q/2)$, to get

$$\frac{\partial(a_3)_{\alpha\mu}(q)}{\partial q^\nu} = (a'_{3,1})_{\alpha\mu\nu}(q) + (a'_{3,2})_{\alpha\mu\nu}(q) + (a'_{3,3})_{\alpha\mu\nu}(q), \tag{4.9}$$

with

$$\begin{aligned}(a'_{3,1})_{\alpha\mu\nu}(q) &= -2\lambda\int_k k_\alpha\left[\frac{\partial}{\partial q^\nu}D(k-u)\right]D(k+u) \\ &\quad\times\widetilde{\Gamma}_\mu(k+u,u-k,-q), \\ (a'_{3,2})_{\alpha\mu\nu}(q) &= -2\lambda\int_k k_\alpha D(k-u)\left[\frac{\partial}{\partial q^\nu}D(k+u)\right] \\ &\quad\times\widetilde{\Gamma}_\mu(k+u,u-k,-q), \\ (a'_{3,3})_{\alpha\mu\nu}(q) &= -2\lambda\int_k k_\alpha D(k-u)D(k+u) \\ &\quad\times\left[\frac{\partial}{\partial q^\nu}\widetilde{\Gamma}_\mu(k+u,u-k,-q)\right];\end{aligned} \tag{4.10}$$

the last three contributions are depicted graphically in the first line of Fig. 9.

Next, for the terms $(a'_{3,1})_{\alpha\mu\nu}(q)$ and $(a'_{3,2})_{\alpha\mu\nu}(q)$ we use Eq. (4.4) to write

$(a'_{3,1})_{\alpha\mu\nu}(q)$

$$
\begin{aligned}
&= -\lambda \int_k k_\alpha \left[D(k-u)\widetilde{\Gamma}_\nu(k-u,u-k,0)D(k-u)\right] \\
&\quad \times D(k+u)\widetilde{\Gamma}_\mu(k+u,u-k,-q), \\
&(a'_{3,2})_{\alpha\mu\nu}(q) \\
&= -\lambda \int_k k_\alpha D(k-u)\left[D(k+u)\widetilde{\Gamma}_\nu(k+u,-u-k,0)\right. \\
&\quad \left. \times D(k+u)\right]\widetilde{\Gamma}_\mu(k+u,u-k,-q). \qquad (4.11)
\end{aligned}
$$

A direct comparison of these last expressions with the contributions to $(c_3)_{\alpha\mu\nu}(q,-q,0)$ in Eq. (3.23) [for $(q,r,p)\to(q,-q,0)$] allows one to establish that

$$
\begin{aligned}
(a'_{3,1})_{\alpha\mu\nu}(q) &= (c_{3,1})_{\alpha\mu\nu}(q,-q,0), \\
(a'_{3,2})_{\alpha\mu\nu}(q) &= (c_{3,2})_{\alpha\mu\nu}(q,-q,0). \qquad (4.12)
\end{aligned}
$$

Consider finally the $(c_{3,3})^{abc}_{\alpha\mu\nu}$ in Eq. (3.24); setting $(q,r,p)\to(q,-q,0)$, shifting $k\to u-k$, and employing Eq. (4.6), we get

$$
\begin{aligned}
(c_{3,3})^{abc}_{\alpha\mu\nu}(q,-q,0) &= 2g^2 f^{eda}\int_k k_\alpha D(k-u)D(k+u) \\
&\quad \times \widehat{\Gamma}^{bcde}_{\mu\nu}(-q,0,k+u,u-k), \\
&= -\frac{\lambda}{2}\int_k k_\alpha D(k-u)D(k+u)\left(\frac{\partial}{\partial(k+u)^\nu}+\frac{\partial}{\partial(u-k)^\nu}\right) \\
&\quad \times \widetilde{\Gamma}_\mu(k+u,u-k,-q), \\
&= -2\lambda\int_k k_\alpha D(k-u)D(k+u)\frac{\partial}{\partial q^\nu} \\
&\quad \times \widetilde{\Gamma}_\mu(k+u,u-k,-q), \qquad (4.13)
\end{aligned}
$$

and therefore

$$
(a'_{3,3})_{\alpha\mu\nu}(q) = (c_{3,3})_{\alpha\mu\nu}(q,-q,0), \qquad (4.14)
$$

which completes the proof of Eq. (4.8). The interpretation of the previous steps in terms of background-gluon insertions is given in the second line of Fig. 9.

5 Discussion and conclusions

It has been known for some time [66] that the transversality of the background self-energy is enforced in a special way, namely independently for each one of the four subsets (blocks) of diagrams comprising the corresponding SDE. In the present work we have shown that the Abelian STI of the background three-gluon vertex is also realized according to the exact same pattern, at the level of the corresponding SDE: the momentum contraction of each subset of vertex diagrams generates the difference of the corresponding self-energy subsets.

The demonstration of this property has been carried out at the level of the fully dressed Feynman diagrams that comprise the relevant SDEs. In particular, the contraction of all three-gluon vertex diagrams by the appropriate momentum triggers STIs satisfied by the vertices and the kernels embedded in them, giving rise to crucial rearrangements and cancellations, which are implemented algebraically, with no need to resort to any integrations. Note that the extensive reorganization of diagrams observed here has been first identified in the context of the pinch technique [5,82–85], where the "gauge-invariant" three-gluon vertex was first studied at the one-loop level [77,86,87]. Evidently, it would be particularly interesting to explore the origin of the block-wise STIs at a formal level, and establish its validity by means of the Batalin–Vilkovisky functional machinery [5,88–92].

It is natural to conjecture that the STI of the background four-gluon vertex, B^4, given by [86,93]

$$
\begin{aligned}
q^\mu \widehat{\mathbf{\Gamma}}^{mnrs}_{\mu\alpha\beta\gamma}(q,r,p,t) &= f^{mse}f^{ern}\widehat{\mathbf{\Gamma}}_{\alpha\beta\gamma}(r,p,q+t) \\
&\quad + f^{mne}f^{esr}\widehat{\mathbf{\Gamma}}_{\beta\gamma\alpha}(p,t,q+r) \\
&\quad + f^{mre}f^{ens}\widehat{\mathbf{\Gamma}}_{\gamma\alpha\beta}(t,r,q+p), \qquad (5.1)
\end{aligned}
$$

is realized according to the same block-wise pattern described above. A diagrammatic demonstration along the lines presented in this work appears to be quite feasible, and would give further support to the notion that the STI of any B^n-type of vertex is enforced in this characteristic manner.

Some of the results presented in Sect. 4 may be used in order to explore the numerical impact of certain truncations or approximations, in the spirit of the recent study presented in [94]. For example, the equality shown in Fig. 9 will be distorted if the vertex $\mathrm{BB}\bar{c}\mathrm{c}$ were to be replaced by its tree level value, given by Eq. (B6). The amount of discrepancy induced between the two sides of this equation is a quantitative indicator of the veracity of such an approximation.

Throughout the present analysis we have assumed that the BBB vertex does not contain irregularities in the form of massless poles. However, as has been shown in detail in a series of studies, the emergence of a dynamical gluon mass [82] through the operation of the Schwinger mechanism [95,96] hinges on the inclusion of longitudinally coupled massless poles in the fundamental vertices of the theory [67,97–102] Quite importantly: (*a*) the STIs satisfied by the vertices are resolved with the nontrivial participation of these poles, and (*b*) in the soft-gluon limit, the associated WIs are *displaced* by an amount controlled by the corresponding pole residues [101,103,104]. In particular, ongoing research reveals that the STIs impose stringent conditions on the pole content of the three-gluon vertex, which must, at the same time, be dynamically realized. The treatment of this problem within the BFM (i.e., at the level of the BBB rather than the QQQ vertex) eliminates structures originating from the ghost-sector of the theory, which tend to complicate and obscure the underlying physical picture. We expect that the completion of this study will shed light on the question of

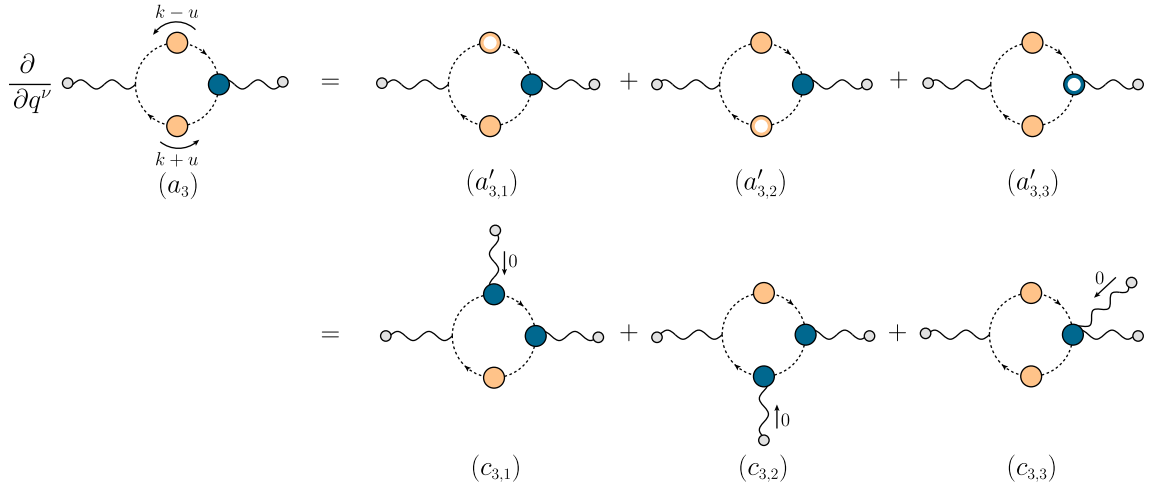

Fig. 9 The diagrammatic representation of the differentiation of the graph (a_3) with respect to q^ν. The effect of differentiating the ghost propagator (dressed background ghost-gluon vertex) is the insertion of a zero-momentum background gluon leg in the propagator (vertex)

how symmetry-induced constraints are dynamically enforced at the level the corresponding SDEs.

Acknowledgements The work of A. C. A. and B. M. O. are supported by the CNPq grants 307854/2019-1 and 141409/2021-5, respectively. A. C. A also acknowledges financial support from project 464898/2014-5 (INCT-FNA). M. N. F. and J. P. are supported by the Spanish MICINN grant PID2020-113334GB-I00. M. N. F. acknowledges financial support from Generalitat Valenciana through contract CIAPOS/2021/74. J. P. also acknowledges funding from the regional Prometeo/2019/087 from the Generalitat Valenciana.

Data Availability Statement This manuscript has no associated data or the data will not be deposited. [Authors' comment: All data generated or analyzed during this study are included in this published article.]

Funded by SCOAP[3]. SCOAP[3] supports the goals of the International Year of Basic Sciences for Sustainable Development.

Appendix A: Derivation of Abelian STIs

In this Appendix we employ the Batalin–Vilkovisky formalism [5,88–92] to derive the Abelian STI satisfied by the generic vertex BQ^n when contracted by the momentum carried by the gluon B.

We start with the WI functional, given by [5]

$$W = \int d^4x \left[\delta_\vartheta Q^{x,\mu}(x) \frac{\delta\Gamma}{\delta Q^x_\mu(x)} + \delta_\vartheta B^{x,\mu}(x) \frac{\delta\Gamma}{\delta B^x_\mu(x)} + \delta_\vartheta c^x(x) \frac{\delta\Gamma}{\delta c^x(x)} + \delta_\vartheta \bar{c}^x(x) \frac{\delta\Gamma}{\delta \bar{c}^x(x)} \right] = 0, \tag{A1}$$

where ϑ^a are the local infinitesimal parameters which correspond to the SU(3) generators t^a, and play the role of the ghost field. Γ in Eq. (A1) is the "reduced" effective action, defined as the full effective action without the gauge-fixing term [5,90]. Consequently, the Green's functions obtained from Γ will be missing the corresponding gauge-dependent contribution at tree level. Finally, the gauge transformations of the fields are given by

$$\begin{aligned} &\delta_\vartheta Q^x_\mu = g f^{xdc} Q^d_\mu \vartheta^c, \qquad \delta_\vartheta B^x_\mu = \partial_\mu \vartheta^x + g f^{xdc} B^d_\mu \vartheta^c, \\ &\delta_\vartheta c^x = -g f^{xdc} c^d \vartheta^c, \qquad \delta_\vartheta \bar{c}^x = -g f^{xdc} \bar{c}^d \vartheta^c. \end{aligned} \tag{A2}$$

To obtain the background Abelian STIs the first step is to differentiate the functional W with respect to the parameter $\vartheta^a(x)$, furnishing

$$\frac{\delta W}{\delta \vartheta^a(x)} = g f^{eda} Q^d_\mu(x) \Gamma_{Q^e_\mu}(x) + \partial_\mu \Gamma_{B^a_\mu}(x) = 0, \tag{A3}$$

where we have already set to zero the vacuum expectation values (VEVs) of the ghost, antighost, and background gluon fields[2]. Moreover, we introduce the shorthand notation for

[2] In the end of the procedure all of the VEVs are set to zero. Since the BQ^n vertex has only one external B and no external ghost and antighost fields these VEVs can be set to zero from the outset.

functional derivatives

$$\Gamma_{\phi_1\phi_2\ldots\phi_n}(x_1,x_2,\ldots,x_n) := \frac{\delta^n\Gamma}{\delta\phi_1(x_1)\delta\phi_2(x_2)\ldots\delta\phi_n(x_n)}, \tag{A4}$$

where $\phi_i(x_i)$ denotes a generic field.

The STIs of interest are then obtained by differentiating Eq. (A3) n times with respect to the quantum gluon. Note, in particular, that the functional derivatives of the term $\partial_\mu\Gamma_{B^a_\mu}(x)$ in Eq. (A3) generate divergences such as $\partial_\mu\Gamma_{B^a_\mu Q^{b_1}_{\nu_1}\ldots Q^{b_n}_{\nu_n}}(x,y_1,\ldots,y_n)$ which, after Fourier transformation, result in the typical l.h.s. of the Abelian STIs, i.e., a Green's function contracted with a background gluon momentum.

To fix the ideas, let us consider as two special cases the STIs for the BQ and BQQ functions.

Differentiating Eq. (A3) with respect to $Q^{b_1}_{\nu_1}(y_1)$ we obtain

$$\begin{aligned}\frac{\delta^2 W}{\delta Q^{b_1}_{\nu_1}(y_1)\delta\vartheta^a(x)} &= gf^{eb_1a}\delta(x-y_1)\Gamma_{Q^e_{\nu_1}}(x)\\ &+ gf^{eda}\,Q^d_\mu(x)\Gamma_{Q^{b_1}_{\nu_1}Q^e_\mu}(y_1,x)\\ &+ \partial_\mu\Gamma_{B^a_\mu Q^{b_1}_{\nu_1}}(x,y_1) = 0.\end{aligned} \tag{A5}$$

Setting the gluon field $Q=0$, and the one-point function $\Gamma_{Q^e_{\nu_1}}(x)=0$, we obtain

$$\partial_\mu\Gamma_{B^a_\mu Q^{b_1}_{\nu_1}}(x,y_1) = 0, \tag{A6}$$

where $\Gamma_{B^a_\mu Q^{b_1}_{\nu_1}}(x,y_1)$ is the inverse BQ propagator, with its $1/\xi_Q$ term removed. In momentum space notation, Eq. (A6) becomes

$$q^\mu\left[q^2P_{\mu\nu}(q)+i\widetilde{\Pi}_{\mu\nu}(q)\right]=0 \quad\Longrightarrow\quad q^\mu\widetilde{\Pi}_{\mu\nu}(q)=0, \tag{A7}$$

expressing the exact transversality of the BQ self-energy.

Then, an additional differentiation of Eq. (A5) with respect to $Q^{b_2}_{\nu_2}(y_2)$ yields

$$\begin{aligned}&\frac{\delta^3 W}{\delta Q^{b_2}_{\nu_2}(y_1)\delta Q^{b_1}_{\nu_1}(y_1)\delta\vartheta^a(x)}\\ &= gf^{eb_1a}\delta(x-y_1)\Gamma_{Q^e_{\nu_1}Q^{b_2}_{\nu_2}}(x,y_2)\\ &+ gf^{eb_2a}\delta(x-y_2)\Gamma_{Q^{b_1}_{\nu_1}Q^e_{\nu_2}}(y_1,x)\\ &+ gf^{eda}\,Q^d_\mu(x)\Gamma_{Q^{b_1}_{\nu_1}Q^{b_2}_{\nu_2}Q^e_\mu}(y_1,y_2,x)\\ &+ \partial_\mu\Gamma_{B^a_\mu Q^{b_1}_{\nu_1}Q^{b_2}_{\nu_2}}(x,y_1,y_2) = 0.\end{aligned} \tag{A8}$$

At this point, by setting all the fields to zero we obtain the Abelian STI for the BQQ vertex in configuration space, namely

$$\begin{aligned}\partial_\mu\Gamma_{B^a_\mu Q^{b_1}_{\nu_1}Q^{b_2}_{\nu_2}}(x,y_1,y_2) =& -gf^{eab_1}\delta(x-y_1)\Gamma_{Q^e_{\nu_1}Q^{b_2}_{\nu_2}}(x,y_2)\\ &-gf^{eab_2}\delta(x-y_2)\Gamma_{Q^{b_1}_{\nu_1}Q^e_{\nu_2}}(y_1,x).\end{aligned} \tag{A9}$$

Now, Fourier transforming the above equation to momentum space leads to

$$\begin{aligned}q^\mu\Gamma_{B^a_\mu Q^{b_1}_{\nu_1}Q^{b_2}_{\nu_2}}(q,r,p) =& gf^{ab_1b_2}\left[p^2P_{\mu\nu}(p)+\Pi_{\mu\nu}(p)\right]\\ &-gf^{ab_1b_2}\left[r^2P_{\mu\nu}(r)+\Pi_{\mu\nu}(r)\right],\end{aligned} \tag{A10}$$

which, with the definition of Eq. (2.3), becomes Eq. (C1). The derivation of the STI for the BBB vertex, given in Eq. (3.6), is completely analogous.

Next, we prove that the STI of the BQ^n vertex is given by

$$\begin{aligned}&-\partial_\mu\Gamma_{B^a_\mu Q^{b_1}_{\nu_1}Q^{b_2}_{\nu_2}\cdots Q^{b_n}_{\nu_n}}(x,y_1,y_2,\ldots,y_n)\\ &= gf^{eab_1}\delta(x-y_1)\Gamma_{Q^e_{\nu_1}Q^{b_2}_{\nu_2}Q^{b_3}_{\nu_3}\cdots Q^{b_n}_{\nu_n}}(x,y_2,y_3,\ldots,y_n)\\ &\quad+gf^{eab_2}\delta(x-y_2)\Gamma_{Q^{b_1}_{\nu_1}Q^e_{\nu_2}Q^{b_3}_{\nu_3}\cdots Q^{b_n}_{\nu_n}}(y_1,x,y_3,\ldots,y_n)+\cdots\\ &\quad+gf^{eab_n}\delta(x-y_n)\Gamma_{Q^{b_1}_{\nu_1}Q^{b_2}_{\nu_2}\cdots Q^{b_{n-1}}_{\nu_{n-1}}Q^e_{\nu_n}}(y_1,y_2,\ldots,y_{n-1},x).\end{aligned} \tag{A11}$$

To that end, we first differentiate Eq. (A8) $n-2$ times. This procedure yields

$$\begin{aligned}&-\partial_\mu\Gamma_{B^a_\mu Q^{b_1}_{\nu_1}Q^{b_2}_{\nu_2}\cdots Q^{b_n}_{\nu_n}}(x,y_1,y_2,\ldots,y_n)\\ &= gf^{eab_1}\delta(x-y_1)\Gamma_{Q^e_{\nu_1}Q^{b_2}_{\nu_2}Q^{b_3}_{\nu_3}\cdots Q^{b_n}_{\nu_n}}(x,y_2,y_3,\ldots,y_n)\\ &\quad+gf^{eab_2}\delta(x-y_2)\Gamma_{Q^{b_1}_{\nu_1}Q^e_{\nu_2}Q^{b_3}_{\nu_3}\cdots Q^{b_n}_{\nu_n}}(y_1,x,y_3,\ldots,y_n)\\ &\quad+gf^{eax}\left\{\frac{\delta^{n-2}}{\delta Q^{b_n}_{\nu_n}(y_n)\cdots\delta Q^{b_3}_{\nu_3}(y_3)}\right.\\ &\quad\left.\times\left[Q^x_\mu(x)\Gamma_{Q^{b_1}_{\nu_1}Q^{b_2}_{\nu_2}Q^e_\mu}(y_1,y_2,x)\right]\right\}_{Q\to0}.\end{aligned} \tag{A12}$$

Clearly, to demonstrate Eq. (A11) we need to prove that

$$\begin{aligned}&gf^{eax}\left\{\frac{\delta^{n-2}}{\delta Q^{b_n}_{\nu_n}(y_n)\cdots\delta Q^{b_3}_{\nu_3}(y_3)}\left[Q^x_\mu(x)\Gamma_{Q^{b_1}_{\nu_1}Q^{b_2}_{\nu_2}Q^e_\mu}(y_1,y_2,x)\right]\right\}_{Q\to0}\\ &= gf^{eab_3}\delta(x-y_3)\Gamma_{Q^{b_1}_{\nu_1}Q^{b_2}_{\nu_2}Q^e_{\nu_3}Q^{b_4}_{\nu_4}\cdots Q^{b_n}_{\nu_n}}(y_1,y_2,x,y_4,\ldots,y_n)+\cdots\\ &\quad+gf^{eab_n}\delta(x-y_n)\Gamma_{Q^{b_1}_{\nu_1}Q^{b_2}_{\nu_2}\cdots Q^{b_{n-1}}_{\nu_{n-1}}Q^e_{\nu_n}}(y_1,y_2,\ldots,y_{n-1},x)\\ &\quad+gf^{eax}\left[Q^x_\mu(x)\Gamma_{Q^{b_1}_{\nu_1}Q^{b_2}_{\nu_2}\cdots Q^{b_n}_{\nu_n}Q^e_\mu}(y_1,y_2,\ldots,y_n,x)\right]_{Q\to0}.\end{aligned} \tag{A13}$$

The proof proceeds by induction. First, it is clear that Eq. (A13) holds for $n = 3$. Indeed, in this case one has to take a single derivative

$$
\begin{aligned}
& g f^{eax} \left\{ \frac{\delta}{\delta Q^{b_3}_{\nu_3}(y_3)} \left[Q^x_\mu(x) \Gamma_{Q^{b_1}_{\nu_1} Q^{b_2}_{\nu_2} Q^e_\mu}(y_1, y_2, x) \right] \right\}_{Q\to 0} \\
&\quad = g f^{eab_3} \delta(x - y_3) \Gamma_{Q^{b_1}_{\nu_1} Q^{b_2}_{\nu_2} Q^e_{\nu_3}}(y_1, y_2, x) \\
&\qquad + g f^{eax} \left[Q^x_\mu(x) \Gamma_{Q^{b_1}_{\nu_1} Q^{b_2}_{\nu_2} Q^{b_3}_{\nu_3} Q^e_\mu}(y_1, y_2, y_3, x) \right]_{Q\to 0},
\end{aligned}
\tag{A14}
$$

which is Eq. (A13) for $n = 3$.

Then, assume that Eq. (A13) is true for $n = k$. Differentiating the result once more with respect to $Q^{b_{k+1}}_{\nu_{k+1}}$ we obtain

$$
\begin{aligned}
& g f^{eax} \left\{ \frac{\delta^{k-1}}{\delta Q^{b_{k+1}}_{\nu_{k+1}}(y_{k+1}) \delta Q^{b_k}_{\nu_k}(y_k) \cdots \delta Q^{b_3}_{\nu_3}(y_3)} \right. \\
&\quad \left. \times \left[Q^x_\mu(x) \Gamma_{Q^{b_1}_{\nu_1} Q^{b_2}_{\nu_2} Q^e_\mu}(y_1, y_2, x) \right] \right\}_{Q\to 0} \\
&\quad = g f^{eab_3} \delta(x - y_3) \Gamma_{Q^{b_1}_{\nu_1} Q^{b_2}_{\nu_2} Q^e_{\nu_3} Q^{b_4}_{\nu_4} \cdots Q^{b_k}_{\nu_k} Q^{b_{k+1}}_{\nu_{k+1}}} \\
&\qquad \times (y_1, y_2, x, y_4, \ldots, y_k, y_{k+1}) + \cdots \\
&\qquad + g f^{eab_k} \delta(x - y_k) \Gamma_{Q^{b_1}_{\nu_1} Q^{b_2}_{\nu_2} \cdots Q^{b_{k-1}}_{\nu_{k-1}} Q^e_{\nu_k} Q^{b_{k+1}}_{\nu_{k+1}}} \\
&\qquad \times (y_1, y_2, \ldots, y_{k-1}, x, y_{k+1}) \\
&\qquad + g f^{eab_{k+1}} \delta(x - y_{k+1}) \Gamma_{Q^{b_1}_{\nu_1} Q^{b_2}_{\nu_2} \cdots Q^{b_k}_{\nu_k} Q^e_{\nu_{k+1}}} \\
&\qquad \times (y_1, y_2, \ldots, y_k, x). \\
&\qquad + g f^{eax} \left[Q^x_\mu(x) \Gamma_{Q^{b_1}_{\nu_1} Q^{b_2}_{\nu_2} \cdots Q^{b_k}_{\nu_k} Q^{b_{k+1}}_{\nu_{k+1}} Q^e_\mu} \right. \\
&\qquad \left. \times (y_1, y_2, \ldots, y_k, y_{k+1}, x) \right]_{Q\to 0},
\end{aligned}
\tag{A15}
$$

which is Eq. (A13) for $n = k + 1$. This completes the proof.

In momentum space, Eq. (A11) is given by (suppressing a factor of g)

$$
\begin{aligned}
& i q_\mu \Gamma_{B^a_\mu Q^{b_1}_{\nu_1} Q^{b_2}_{\nu_2} \cdots Q^{b_n}_{\nu_n}}(q, p_1, p_2, \ldots, p_n) \\
&\quad = f^{eab_1} \Gamma_{Q^e_{\nu_1} Q^{b_2}_{\nu_2} Q^{b_3}_{\nu_3} \cdots Q^{b_n}_{\nu_n}}(p_1 + q, p_2, p_3, \ldots, p_n) \\
&\qquad + f^{eab_2} \Gamma_{Q^{b_1}_{\nu_1} Q^e_{\nu_2} Q^{b_3}_{\nu_3} \cdots Q^{b_n}_{\nu_n}}(p_1, p_2 + q, p_3, \ldots, p_n) + \cdots \\
&\qquad + f^{eab_n} \Gamma_{Q^{b_1}_{\nu_1} Q^{b_2}_{\nu_2} \cdots Q^{b_{n-1}}_{\nu_{n-1}} Q^e_{\nu_n}}(p_1, p_2, p_3, \ldots, p_n + q).
\end{aligned}
\tag{A16}
$$

The corresponding WI is obtained by expanding Eq. (A16) around $q = 0$ and collecting terms linear in q. Using $p_n = -\sum_{i=1}^{n-1} p_i$, we obtain

$$
\begin{aligned}
& i \Gamma_{B^a_\mu Q^{b_1}_{\nu_1} Q^{b_2}_{\nu_2} \cdots Q^{b_n}_{\nu_n}}(0, p_1, p_2, \ldots, p_n) \\
&\quad = \left(f^{eab_1} \frac{\partial}{\partial p_1^{\nu_1}} + \cdots + f^{eab_{n-1}} \frac{\partial}{\partial p_{n-1}^{\nu_{n-1}}} \right) \\
&\qquad \times \Gamma_{Q^{b_1}_{\nu_1} \cdots Q^e_{\nu_n}}(p_1, \ldots, p_n).
\end{aligned}
\tag{A17}
$$

Note that the absence of a zeroth order term on the l.h.s. of Eq. (A16) implies the relation

$$
\begin{aligned}
0 = & f^{eab_1} \Gamma_{Q^e_{\nu_1} Q^{b_2}_{\nu_2} Q^{b_3}_{\nu_3} \cdots Q^{b_n}_{\nu_n}}(p_1, p_2, p_3, \ldots, p_n) \\
& + f^{eab_2} \Gamma_{Q^{b_1}_{\nu_1} Q^e_{\nu_2} Q^{b_3}_{\nu_3} \cdots Q^{b_n}_{\nu_n}}(p_1, p_2, p_3, \ldots, p_n) + \cdots \\
& + f^{eab_n} \Gamma_{Q^{b_1}_{\nu_1} Q^{b_2}_{\nu_2} \cdots Q^{b_{n-1}}_{\nu_{n-1}} Q^e_{\nu_n}}(p_1, p_2, p_3, \ldots, p_n),
\end{aligned}
\tag{A18}
$$

whose validity we have checked explicitly for $n = 3, 4$.

Appendix B: Feynman rules for BFM vertices

In the Table 1 of this Appendix we list the Feynman rules for BFM vertices at tree level.

Table 1 The diagrammatic representations of the new vertices appearing in the BFM and their respective Feynman rules at tree level [5]. Notice that for the three-point functions we have factored out the coupling g and their respective color structure, following the definitions of Eq. (2.3), while for the four-point functions, we have factored out only $-ig^2$ as shown in Eq. (2.4)

Vertex	Feynman rule
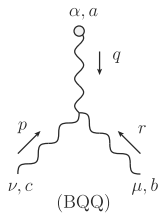	$\widetilde{\Gamma}^{(0)}_{\alpha\mu\nu}(q,r,p) = (q-r)_\nu g_{\alpha\mu} + (r-p)_\alpha g_{\mu\nu} + (p-q)_\mu g_{\alpha\nu} + \xi_Q^{-1}(g_{\alpha\nu} r_\mu - g_{\alpha\mu} p_\nu)\,,$ (B1)
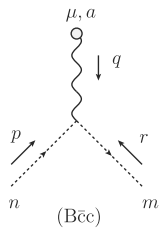	$\widetilde{\Gamma}^{(0)}_{\mu}(r,p,q) = (r-p)_\mu\,,$ (B2)
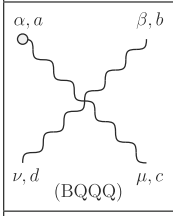	$\widetilde{\Gamma}^{(0)abcd}_{\alpha\beta\mu\nu} = f^{adx} f^{cbx}\,(g_{\alpha\mu} g_{\beta\nu} - g_{\alpha\beta} g_{\mu\nu}) + f^{abx} f^{dcx}\,(g_{\alpha\nu} g_{\beta\mu} - g_{\alpha\mu} g_{\beta\nu}) + f^{acx} f^{dbx}\,(g_{\alpha\nu} g_{\beta\mu} - g_{\alpha\beta} g_{\mu\nu})\,,$ (B3)
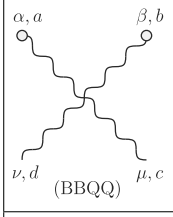	$\widehat{\Gamma}^{(0)abcd}_{\alpha\beta\mu\nu} = \Gamma^{(0)abcd}_{\alpha\beta\mu\nu} + \xi_Q^{-1}(f^{adx} f^{bcx} g_{\alpha\nu} g_{\beta\mu} - f^{acx} f^{dbx} g_{\alpha\mu} g_{\beta\nu})\,,$ (B4)
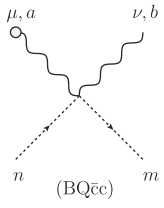	$\widetilde{\Gamma}^{(0)abmn}_{\mu\nu} = f^{max} f^{xbn} g_{\mu\nu}\,,$ (B5)
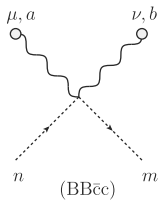	$\widehat{\Gamma}^{(0)abmn}_{\mu\nu} = g_{\mu\nu}\left(f^{max} f^{bnx} + f^{mbx} f^{anx}\right)\,.$ (B6)

Appendix C: Abelian Slavnov–Taylor identities in the BFM

In the Table 2 we collect all the Abelian STI in the BFM necessary to demonstrate the block-wise realization of the STI for the background three-gluon vertex.

Appendix D: Expressions for the two-loop ghost sector of the BBB SDE

The two-loop ghost sector of the SDE of the vertex BBB given by diagram (e) in Fig. 2, whose expansion is given in Fig. 6, relate with the background gluon self-energy by Eq. (3.43), where the expression for the diagrams (a_7), (a_8), (a_9) and (a_{10}), in Fig. 1 can be expressed as

$$(a_7)^{ab}_{\alpha\mu}(q) = ig^4 h_1^{aedm}\int_k\int_l D(l)D(s)\Delta^{\beta}_{\alpha}(k) \times \widetilde{\Gamma}^{bmde}_{\mu\beta}(-q,k,l,s), \tag{D1}$$

$$(a_8)^{ab}_{\alpha\mu}(q) = \frac{1}{2}i\lambda^2\delta^{ab}g_{\alpha\beta}\int_k\int_l R_{\sigma}(-l,l-k) \times \widetilde{R}^{\sigma\beta}_{\mu}(-k,q+k), \tag{D2}$$

$$(a_9)^{ab}_{\alpha\mu}(q) = -i\lambda^2\delta^{ab}\int_k\int_l D(q+l)\Delta^{\beta}_{\alpha}(k)R_{\beta}(k-l,l) \times \widetilde{\Gamma}_{\mu}(-l,q+l,-q), \tag{D3}$$

$$(a_{10})^{ab}_{\alpha\mu}(q) = -\frac{1}{2}i\lambda^2\delta^{ab}\int_k\int_l D(q+l)\Delta^{\beta}_{\alpha}(k) \times R_{\beta}(l,k-l)\widetilde{\Gamma}_{\mu}(q+l,-l,-q). \tag{D4}$$

The decomposition of diagram (e), given in Eqs. (3.41) and (3.42), can be separated in three groups: $(e_1)^{abc}_{\alpha\mu\nu}$, with

$$\begin{aligned}
(e_{1,1})^{abc}_{\alpha\mu\nu} &= ig^4 h_2^{amdce}g_{\alpha\beta}\int_k\int_l D(k)D(s)\widetilde{R}^{\beta\sigma}_{\nu}(l,-p-l) \times \widetilde{\Gamma}^{bedm}_{\mu\sigma}(r,l+p,s,k),\\
(e_{1,2})^{abc}_{\alpha\mu\nu} &= ig^4 h_2^{cmade}\int_k\int_l D(s)\Delta^{\beta}_{\alpha}(l)\widetilde{R}_{\nu}(-p-k,k) \times \widetilde{\Gamma}^{bedm}_{\mu\beta}(r,l,s,k+p),\\
(e_{1,3})^{abc}_{\alpha\mu\nu} &= ig^4 h_2^{amecd}\int_k\int_l D(k)\Delta^{\beta}_{\alpha}(l)\widetilde{R}_{\nu}(k,-k-p) \times \widetilde{\Gamma}^{bedm}_{\mu\beta}(r,l,k+p,s),\\
(e_{1,4})^{abc}_{\alpha\mu\nu} &= ig^4 h_1^{amed}\int_k\int_l D(k)D(s)\Delta^{\beta}_{\alpha}(l)\widehat{\Gamma}^{bcedm}_{\mu\nu\beta}(r,p,l,s,k),
\end{aligned} \tag{D5}$$

$(e_2)^{abc}_{\alpha\mu\nu}$, with

$$\begin{aligned}
(e_{2,1})^{abc}_{\alpha\mu\nu} &= ig^4 h_2^{amebd}g_{\alpha\beta}\int_k\int_l D(k)D(s)\widetilde{R}^{\beta\sigma}_{\mu}(l,-r-l) \times \widetilde{\Gamma}^{cdem}_{\nu\sigma}(p,r+l,s,k),\\
(e_{2,2})^{abc}_{\alpha\mu\nu} &= -\frac{i}{4}\lambda^2 f^{abc}\int_k\int_l \Delta^{\beta}_{\alpha}(l)R_{\rho}(s,k)\widetilde{R}^{\sigma\rho}_{\mu}(p+l,q-l) \times \widetilde{\Gamma}_{\nu\beta\sigma}(p,l,-p-l),\\
(e_{2,3})^{abc}_{\alpha\mu\nu} &= -\frac{i}{4}\lambda^2 f^{abc}g_{\alpha\beta}\int_k\int_l \Delta^{\lambda\rho}(q-l)R_{\lambda}(s,k) \times \widetilde{R}^{\beta\sigma}_{\mu}(l,-r-l)\widetilde{\Gamma}_{\nu\rho\sigma}(p,q-l,l+r),\\
(e_{2,4})^{abc}_{\alpha\mu\nu} &= \frac{i}{4}\lambda^2 f^{abc}g_{\alpha\beta}\int_k\int_l D(s) \times \widetilde{R}_{\nu}(-k-p,k)\widetilde{R}^{\beta\sigma}_{\mu}(l,-r-l)\Gamma_{\sigma}(s,k+p,l+r),\\
(e_{2,5})^{abc}_{\alpha\mu\nu} &= ig^4 h_1^{xmbe}h_2^{amecx}g_{\alpha\beta}\int_k\int_l D(s)\widetilde{R}_{\nu}(k,-k-p) \times \widetilde{R}^{\beta\sigma}_{\mu}(l,-r-l)\Gamma_{\sigma}(k+p,s,l+r),\\
(e_{2,6})^{abc}_{\alpha\mu\nu} &= \frac{i}{2}g^2\lambda f^{aem}\int_k\int_l \Delta^{\beta}_{\alpha}(l)\Delta^{\rho\sigma}(q-l)R_{\rho}(s,k) \times \widehat{\Gamma}^{bcem}_{\mu\nu\beta\sigma}(r,p,l,q-l),
\end{aligned} \tag{D6}$$

and finally $(e_3)^{abc}_{\alpha\mu\nu}$, with

$$\begin{aligned}
(e_{3,1})^{abc}_{\alpha\mu\nu} &= ig^4 h_2^{bmade}\int_k\int_l D(s)\Delta^{\beta}_{\alpha}(l)\widetilde{R}_{\mu}(-k-r,k) \times \widetilde{\Gamma}^{cedm}_{\nu\beta}(p,l,s,k+r),\\
(e_{3,2})^{abc}_{\alpha\mu\nu} &= ig^4 h_1^{xmce}h_2^{amebx}g_{\alpha\beta}\int_k\int_l D(k)\widetilde{R}^{\beta\sigma}_{\nu}(l,-l-p) \times R_{\sigma}(s,k+r)\widetilde{\Gamma}_{\mu}(-k-r,k,r),\\
(e_{3,3})^{abc}_{\alpha\mu\nu} &= -\frac{i}{4}\lambda^2 f^{abc}\int_k\int_l \Delta^{\beta}_{\alpha}(l)\widetilde{R}_{\nu}(k,-k-p) \times R_{\beta}(k-q,s)\widetilde{\Gamma}_{\mu}(k+p,q-k,r),\\
(e_{3,4})^{abc}_{\alpha\mu\nu} &= -\frac{i}{4}\lambda^2 f^{abc}\int_k\int_l \Delta^{\beta}_{\alpha}(l)\Gamma_{\beta}(s+p,k+r,l) \times \widetilde{R}_{\mu}(-k-r,k)\widetilde{R}_{\nu}(s,-s-p),\\
(e_{3,5})^{abc}_{\alpha\mu\nu} &= -\frac{i}{2}\lambda^2 f^{abc}\int_k\int_l \Delta^{\beta}_{\alpha}(l)R_{\beta}(s,k-q)\widetilde{R}_{\mu}(-k-r,k) \times \widetilde{\Gamma}_{\nu}(q-k,k+r,p),\\
(e_{3,6})^{abc}_{\alpha\mu\nu} &= -\frac{i}{2}g^2\lambda f^{ade}\int_k\int_l D(k)\Delta^{\beta}_{\alpha}(l)R_{\beta}(k-q,s) \times \widehat{\Gamma}^{cbde}_{\mu\nu}(r,p,k,q-k),\\
(e_{3,7})^{abc}_{\alpha\mu\nu} &= ig^4 h_2^{amedb}\int_k\int_l D(s)\Delta^{\beta}_{\alpha}(l)\widetilde{R}_{\mu}(k,-k-r) \times \widetilde{\Gamma}^{cedm}_{\nu\beta}(p,l,k+r,s),\\
(e_{3,8})^{abc}_{\alpha\mu\nu} &= ig^4 h_1^{xmce}h_2^{amebx}g_{\alpha\beta}\int_k\int_l D(k)\widetilde{R}^{\beta\sigma}_{\nu}(l,-l-p) \times R_{\sigma}(k+r,s)\widetilde{\Gamma}_{\mu}(k,-k-r,r),\\
(e_{3,9})^{abc}_{\alpha\mu\nu} &= \frac{i}{2}\lambda^2 f^{abc}\int_k\int_l \Delta^{\beta}_{\alpha}(l)R_{\beta}(s,k-q) \times \widetilde{\Gamma}_{\mu}(q-k,k+p,r)\widetilde{R}_{\nu}(-p-k,k),\\
(e_{3,10})^{abc}_{\alpha\mu\nu} &= \frac{i}{4}\lambda^2 f^{abc}\int_k\int_l \Delta^{\beta}_{\alpha}(l)\Gamma_{\beta}(r-k,-t,l) \times \widetilde{R}_{\mu}(-k,k-r)\widetilde{R}_{\nu}(t,q+k+l),\\
(e_{3,11})^{abc}_{\alpha\mu\nu} &= \frac{i}{2}\lambda^2 f^{abc}\int_k\int_l \Delta^{\beta}_{\alpha}(l)R_{\beta}(k-q,s)
\end{aligned}$$

Table 2 The Abelian STIs satisfied by the BQQ, B$\bar{c}$c, BQQQ, BBQQ, BQ$\bar{c}$c, BB$\bar{c}$c, BBQQQ and BBQ$\bar{c}$c vertices

Vertex	Abelian STI	
BQQ	$q^\alpha \widetilde{\Gamma}_{\alpha\mu\nu}(q,r,p) = \Delta^{-1}_{\mu\nu}(p) - \Delta^{-1}_{\mu\nu}(r),$	(C1)
B$\bar{c}$c	$q^\mu \widetilde{\Gamma}_{\mu}(r,p,q) = D^{-1}(p) - D^{-1}(r),$	(C2)
BQQQ	$q^\alpha \widetilde{\Gamma}^{abcd}_{\alpha\beta\mu\nu}(q,r,p,t) = f^{abx} f^{dcx} \Gamma_{\beta\mu\nu}(r+q,p,t) + f^{acx} f^{bdx} \Gamma_{\beta\mu\nu}(r,p+q,t) + f^{adx} f^{cbx} \Gamma_{\beta\mu\nu}(r,p,t+q),$	(C3)
BBQQ	$q^\alpha \widehat{\Gamma}^{abcd}_{\alpha\beta\mu\nu}(q,r,p,t) = f^{abx} f^{dcx} \widetilde{\Gamma}_{\beta\mu\nu}(r+q,p,t) + f^{acx} f^{bdx} \widetilde{\Gamma}_{\beta\mu\nu}(r,p+q,t) + f^{adx} f^{cbx} \widetilde{\Gamma}_{\beta\mu\nu}(r,p,t+q),$	(C4)
BQ$\bar{c}$c	$q^\mu \widetilde{\Gamma}^{abmn}_{\mu\nu}(q,r,p,t) = f^{nax} f^{bmx} \Gamma_\nu(p,q+t,r) + f^{nbx} f^{max} \Gamma_\nu(q+p,t,r) + f^{nmx} f^{abx} \Gamma_\nu(p,t,q+r),$	(C5)
BB$\bar{c}$c	$q^\mu \widehat{\Gamma}^{abmn}_{\mu\nu}(q,r,p,t) = f^{abx} f^{mnx} \widetilde{\Gamma}_\nu(p,t,q+r) + f^{amx} f^{nbx} \widetilde{\Gamma}_\nu(q+p,t,r) + f^{anx} f^{bmx} \widetilde{\Gamma}_\nu(p,q+t,r),$	(C6)
BBQQQ	$q^\alpha \widehat{\Gamma}^{abcde}_{\alpha\beta\mu\nu\rho}(q,r,p,t,u) = f^{bax} \widetilde{\Gamma}^{xcde}_{\beta\mu\nu\rho}(r+q,p,t,u) + f^{cax} \widetilde{\Gamma}^{bxde}_{\beta\mu\nu\rho}(r,p+q,t,u) + f^{dax} \widetilde{\Gamma}^{bcxe}_{\beta\mu\nu\rho}(r,p,t+q,u) + f^{eax} \widetilde{\Gamma}^{bcdx}_{\beta\mu\nu\rho}(r,p,t,u+q),$	(C7)
BBQ$\bar{c}$c	$q^\alpha \widehat{\Gamma}^{abcmn}_{\alpha\mu\nu}(q,r,p,t,u) = f^{bax} \widetilde{\Gamma}^{xcmn}_{\mu\nu}(r+q,p,t,u) + f^{cax} \widetilde{\Gamma}^{bxmn}_{\mu\nu}(r,p+q,t,u) + f^{max} \widetilde{\Gamma}^{bcxn}_{\mu\nu}(r,p,t+q,u) + f^{nax} \widetilde{\Gamma}^{bcmx}_{\mu\nu}(r,p,t,u+q).$	(C8)

$$\times \widetilde{R}_\mu(k,-k-r)\widetilde{\Gamma}_\nu(k+r,q-k,p),$$

$$(e_{3,12})^{abc}_{\alpha\mu\nu} = -ig^2\lambda f^{ade} \int_k \int_l D(k)\Delta^\beta_\alpha(l) R_\beta(s,k-q) \times \widehat{\Gamma}^{bcde}_{\mu\nu}(r,p,q-k,k). \quad \text{(D7)}$$

References

1. C.D. Roberts, A.G. Williams, Prog. Part. Nucl. Phys. **33**, 477 (1994). https://doi.org/10.1016/0146-6410(94)90049-3
2. R. Alkofer, L. von Smekal, Phys. Rep. **353**, 281 (2001). https://doi.org/10.1016/S0370-1573(01)00010-2
3. C.S. Fischer, J. Phys. G **32**, R253 (2006). https://doi.org/10.1088/0954-3899/32/8/R02
4. C.D. Roberts, Prog. Part. Nucl. Phys. **61**, 50 (2008). https://doi.org/10.1016/j.ppnp.2007.12.034
5. D. Binosi, J. Papavassiliou, Phys. Rep. **479**, 1 (2009). https://doi.org/10.1016/j.physrep.2009.05.001
6. D. Binosi, L. Chang, J. Papavassiliou, C.D. Roberts, Phys. Lett. B **742**, 183 (2015). https://doi.org/10.1016/j.physletb.2015.01.031
7. I.C. Cloet, C.D. Roberts, Prog. Part. Nucl. Phys. **77**, 1 (2014). https://doi.org/10.1016/j.ppnp.2014.02.001
8. A.C. Aguilar, D. Binosi, J. Papavassiliou, Front. Phys. (Beijing) **11**, 111203 (2016). https://doi.org/10.1007/s11467-015-0517-6
9. D. Binosi, L. Chang, J. Papavassiliou, S.-X. Qin, C.D. Roberts, Phys. Rev. D **93**, 096010 (2016). https://doi.org/10.1103/PhysRevD.93.096010
10. D. Binosi, C. Mezrag, J. Papavassiliou, C.D. Roberts, J. Rodriguez-Quintero, Phys. Rev. D **96**, 054026 (2017). https://doi.org/10.1103/PhysRevD.96.054026
11. M.Q. Huber, Phys. Rep. **879**, 1 (2020). https://doi.org/10.1016/j.physrep.2020.04.004
12. J. Papavassiliou, Chin. Phys. C **46**, 112001 (2022). https://doi.org/10.1088/1674-1137/ac84ca
13. P. Maris, C.D. Roberts, Phys. Rev. C **56**, 3369 (1997). https://doi.org/10.1103/PhysRevC.56.3369
14. P. Maris, C.D. Roberts, Int. J. Mod. Phys. E **12**, 297 (2003). https://doi.org/10.1142/S0218301303001326
15. J. Braun, H. Gies, J.M. Pawlowski, Phys. Lett. B **684**, 262 (2010). https://doi.org/10.1016/j.physletb.2010.01.009
16. G. Eichmann, I.C. Cloet, R. Alkofer, A. Krassnigg, C.D. Roberts, Phys. Rev. C **79**, 012202 (2009). https://doi.org/10.1103/PhysRevC.79.012202
17. I. Cloet, G. Eichmann, B. El-Bennich, T. Klahn, C. Roberts, Few Body Syst. **46**, 1 (2009). https://doi.org/10.1007/s00601-009-0015-x
18. P. Boucaud, J.P. Leroy, A. Le Yaouanc, J. Micheli, O. Pene, J. Rodriguez-Quintero, JHEP **06**, 099 (2008). https://doi.org/10.1088/1126-6708/2008/06/099
19. G. Eichmann, R. Alkofer, A. Krassnigg, D. Nicmorus, Phys. Rev. Lett. **104**, 201601 (2010). https://doi.org/10.1103/PhysRevLett.104.201601
20. C.S. Fischer, A. Maas, J.M. Pawlowski, Ann. Phys. **324**, 2408 (2009). https://doi.org/10.1016/j.aop.2009.07.009
21. D. Dudal, J.A. Gracey, S.P. Sorella, N. Vandersickel, H. Verschelde, Phys. Rev. D **78**, 065047 (2008). https://doi.org/10.1103/PhysRevD.78.065047
22. J. Rodriguez-Quintero, J. High Energy Phys. **01**, 105 (2011). https://doi.org/10.1007/JHEP01(2011)105
23. M. Tissier, N. Wschebor, Phys. Rev. D **82**, 101701 (2010). https://doi.org/10.1103/PhysRevD.82.101701
24. M.R. Pennington, D.J. Wilson, Phys. Rev. D **84**, 119901 (2011). https://doi.org/10.1103/PhysRevD.84.119901, https://doi.org/10.1103/PhysRevD.84.094028
25. M.Q. Huber, A. Maas, L. von Smekal, J. High Energy Phys. **11**, 035 (2012). https://doi.org/10.1007/JHEP11(2012)035
26. L. Fister, J.M. Pawlowski, Phys. Rev. D **88**, 045010 (2013). https://doi.org/10.1103/PhysRevD.88.045010
27. A.K. Cyrol, M.Q. Huber, L. von Smekal, Eur. Phys. J. C **75**, 102 (2015). https://doi.org/10.1140/epjc/s10052-015-3312-1
28. J.M. Pawlowski, D.F. Litim, S. Nedelko, L. von Smekal, Phys. Rev. Lett. **93**, 152002 (2004). https://doi.org/10.1103/PhysRevLett.93.152002
29. J.M. Pawlowski, Ann. Phys. **322**, 2831 (2007). https://doi.org/10.1016/j.aop.2007.01.007
30. A.K. Cyrol, M. Mitter, J.M. Pawlowski, N. Strodthoff, Phys. Rev. D **97**, 054006 (2018). https://doi.org/10.1103/PhysRevD.97.054006
31. A.K. Cyrol, J.M. Pawlowski, A. Rothkopf, N. Wink, SciPost Phys. **5**, 065 (2018). https://doi.org/10.21468/SciPostPhys.5.6.065

32. L. Corell, A.K. Cyrol, M. Mitter, J.M. Pawlowski, N. Strodthoff, SciPost Phys. **5**, 066 (2018). https://doi.org/10.21468/SciPostPhys.5.6.066
33. F. Gao, S.-X. Qin, C.D. Roberts, J. Rodriguez-Quintero, Phys. Rev. D **97**, 034010 (2018). https://doi.org/10.1103/PhysRevD.97.034010
34. M.Q. Huber, Phys. Rev. D **93**, 085033 (2016). https://doi.org/10.1103/PhysRevD.93.085033
35. M.Q. Huber, Phys. Rev. D **101**, 114009 (2020). https://doi.org/10.1103/PhysRevD.101.114009
36. J.-P. Blaizot, J.M. Pawlowski, U. Reinosa, Ann. Phys. **431**, 168549 (2021). https://doi.org/10.1016/j.aop.2021.168549
37. C.D. Roberts, Symmetry **12**, 1468 (2020). https://doi.org/10.3390/sym12091468
38. J. Horak, J. Papavassiliou, J.M. Pawlowski, N. Wink, Phys. Rev. D **104**, 074017 (2021). https://doi.org/10.1103/PhysRevD.104.074017
39. F. Gao, J. Papavassiliou, J.M. Pawlowski, Phys. Rev. D **103**, 094013 (2021). https://doi.org/10.1103/PhysRevD.103.094013
40. A. Cucchieri, A. Maas, T. Mendes, Phys. Rev. D **74**, 014503 (2006). https://doi.org/10.1103/PhysRevD.74.014503
41. A. Cucchieri, T. Mendes, PoS **LATTICE2007**, 297 (2007). https://doi.org/10.22323/1.042.0297
42. I. Bogolubsky, E. Ilgenfritz, M. Muller-Preussker, A. Sternbeck, PoS **LATTICE2007**, 290 (2007). https://doi.org/10.22323/1.042.0290
43. I. Bogolubsky, E. Ilgenfritz, M. Muller-Preussker, A. Sternbeck, Phys. Lett. B **676**, 69 (2009). https://doi.org/10.1016/j.physletb.2009.04.076
44. A. Cucchieri, A. Maas, T. Mendes, Phys. Rev. D **77**, 094510 (2008). https://doi.org/10.1103/PhysRevD.77.094510
45. A. Cucchieri, T. Mendes, Phys. Rev. D **81**, 016005 (2010). https://doi.org/10.1103/PhysRevD.81.016005
46. O. Oliveira, P. Silva, PoS **LAT2009**, 226 (2009). https://doi.org/10.22323/1.091.0226
47. O. Oliveira, P. Bicudo, J. Phys. G **G38**, 045003 (2011). https://doi.org/10.1088/0954-3899/38/4/045003
48. A. Maas, Phys. Rep. **524**, 203 (2013). https://doi.org/10.1016/j.physrep.2012.11.002
49. A. Ayala, A. Bashir, D. Binosi, M. Cristoforetti, J. Rodriguez-Quintero, Phys. Rev. D **86**, 074512 (2012). https://doi.org/10.1103/PhysRevD.86.074512
50. O. Oliveira, P.J. Silva, Phys. Rev. D **86**, 114513 (2012). https://doi.org/10.1103/PhysRevD.86.114513
51. A. Athenodorou, D. Binosi, P. Boucaud, F. De Soto, J. Papavassiliou, J. Rodriguez-Quintero, S. Zafeiropoulos, Phys. Lett. B **761**, 444 (2016). https://doi.org/10.1016/j.physletb.2016.08.065
52. A.G. Duarte, O. Oliveira, P.J. Silva, Phys. Rev. D **94**, 074502 (2016). https://doi.org/10.1103/PhysRevD.94.074502
53. P. Boucaud, F. De Soto, J. Rodríguez-Quintero, S. Zafeiropoulos, Phys. Rev. D **96**, 098501 (2017). https://doi.org/10.1103/PhysRevD.96.098501
54. P. Boucaud, F. De Soto, K. Raya, J. Rodríguez-Quintero, S. Zafeiropoulos, Phys. Rev. D **98**, 114515 (2018). https://doi.org/10.1103/PhysRevD.98.114515
55. A.C. Aguilar, C.O. Ambrósio, F. De Soto, M.N. Ferreira, B.M. Oliveira, J. Papavassiliou, J. Rodríguez-Quintero, Phys. Rev. D **104**, 054028 (2021). https://doi.org/10.1103/PhysRevD.104.054028
56. B.S. DeWitt, Phys. Rev. **162**, 1195 (1967). https://doi.org/10.1103/PhysRev.162.1195
57. J. Honerkamp, Nucl. Phys. B **48**, 269 (1972). https://doi.org/10.1016/0550-3213(72)90063-6
58. R.E. Kallosh, Nucl. Phys. B **78**, 293 (1974). https://doi.org/10.1016/0550-3213(74)90284-3
59. H. Kluberg-Stern, J.B. Zuber, Phys. Rev. D **12**, 482 (1975). https://doi.org/10.1103/PhysRevD.12.482
60. I.Y. Arefeva, L.D. Faddeev, A.A. Slavnov, Teor. Mat. Fiz. **21**, 311 (1974). https://doi.org/10.1007/BF01038094
61. L. Abbott, Nucl. Phys. B **185**, 189 (1981). https://doi.org/10.1016/0550-3213(81)90371-0
62. S. Weinberg, Phys. Lett. B **91**, 51 (1980). https://doi.org/10.1016/0370-2693(80)90660-7
63. L.F. Abbott, Acta Phys. Pol. B **13**, 33 (1982). http://cds.cern.ch/record/130265
64. G.M. Shore, Ann. Phys. **137**, 262 (1981). https://doi.org/10.1016/0003-4916(81)90198-6
65. L.F. Abbott, M.T. Grisaru, R.K. Schaefer, Nucl. Phys. B **229**, 372 (1983). https://doi.org/10.1016/0550-3213(83)90337-1
66. A.C. Aguilar, J. Papavassiliou, J. High Energy Phys. **12**, 012 (2006). https://doi.org/10.1088/1126-6708/2006/12/012
67. A.C. Aguilar, D. Binosi, J. Papavassiliou, Phys. Rev. D **78**, 025010 (2008). https://doi.org/10.1103/PhysRevD.78.025010
68. J. Taylor, Nucl. Phys. B **33**, 436 (1971). https://doi.org/10.1016/0550-3213(71)90297-5
69. A. Slavnov, Theor. Math. Phys. **10**, 99 (1972). https://doi.org/10.1007/BF01090719
70. K. Fujikawa, B.W. Lee, A.I. Sanda, Phys. Rev. D **6**, 2923 (1972). https://doi.org/10.1103/PhysRevD.6.2923
71. W.J. Marciano, H. Pagels, Phys. Rep. **36**, 137 (1978). https://doi.org/10.1016/0370-1573(78)90208-9
72. A.I. Davydychev, P. Osland, L. Saks, Phys. Rev. D **63**, 014022 (2001). https://doi.org/10.1103/PhysRevD.63.014022
73. A.C. Aguilar, J. Papavassiliou, Phys. Rev. D **83**, 014013 (2011). https://doi.org/10.1103/PhysRevD.83.014013
74. A.C. Aguilar, J.C. Cardona, M.N. Ferreira, J. Papavassiliou, Phys. Rev. D **96**, 014029 (2017). https://doi.org/10.1103/PhysRevD.96.014029
75. C. Itzykson, J.B. Zuber, *Quantum Field Theory. International Series in Pure and Applied Physics* (Mcgraw-Hill, New York, 1980)
76. M.E. Peskin, D.V. Schroeder, *An Introduction to Quantum Field Theory* (Addison-Wesley, Reading, 1995)
77. J.M. Cornwall, J. Papavassiliou, Phys. Rev. D **40**, 3474 (1989). https://doi.org/10.1103/PhysRevD.40.3474
78. D. Binosi, J. Papavassiliou, Phys. Rev. D **77**, 061702 (2008). https://doi.org/10.1103/PhysRevD.77.061702
79. D. Binosi, J. Papavassiliou, J. High Energy Phys. **11**, 063 (2008). https://doi.org/10.1088/1126-6708/2008/11/063
80. J.S. Ball, T.-W. Chiu, Phys. Rev. D **22**, 2550 (1980). https://doi.org/10.1103/PhysRevD.22.2550. [Erratum: Phys. Rev. D **23**, 3085 (1981)]
81. A.I. Davydychev, P. Osland, O. Tarasov, Phys. Rev. D **54**, 4087 (1996). https://doi.org/10.1103/PhysRevD.59.109901. [Erratum: Phys. Rev. D **59**, 109901 (1999)]
82. J.M. Cornwall, Phys. Rev. D **26**, 1453 (1982). https://doi.org/10.1103/PhysRevD.26.1453
83. J. Papavassiliou, Phys. Rev. D **41**, 3179 (1990). https://doi.org/10.1103/PhysRevD.41.3179
84. A. Pilaftsis, Nucl. Phys. B **487**, 467 (1997). https://doi.org/10.1016/S0550-3213(96)00686-4
85. D. Binosi, J. Papavassiliou, Phys. Rev. D **66**, 111901 (2002). https://doi.org/10.1103/PhysRevD.66.111901
86. S. Hashimoto, J. Kodaira, Y. Yasui, K. Sasaki, Phys. Rev. D **50**, 7066 (1994). https://doi.org/10.1103/PhysRevD.50.7066
87. M. Binger, S.J. Brodsky, Phys. Rev. D **74**, 054016 (2006). https://doi.org/10.1103/PhysRevD.74.054016
88. I.A. Batalin, G.A. Vilkovisky, Phys. Lett. B **69**, 309 (1977). https://doi.org/10.1016/0370-2693(77)90553-6

89. I.A. Batalin, G.A. Vilkovisky, Phys. Rev. D **28**, 2567 (1983). https://doi.org/10.1103/PhysRevD.28.2567. [Erratum: Phys. Rev. D **30**, 508 (1984)]
90. D. Binosi, J. Papavassiliou, Phys. Rev. D **66**, 025024 (2002). https://doi.org/10.1103/PhysRevD.66.025024
91. D. Binosi, A. Quadri, Phys. Rev. D **85**, 121702 (2012). https://doi.org/10.1103/PhysRevD.85.121702
92. D. Binosi, A. Quadri, Phys. Rev. D **88**, 085036 (2013). https://doi.org/10.1103/PhysRevD.88.085036
93. J. Papavassiliou, Phys. Rev. D **47**, 4728 (1993). https://doi.org/10.1103/PhysRevD.47.4728
94. A.C. Aguilar, M.N. Ferreira, B.M. Oliveira, J. Papavassiliou, Eur. Phys. J. C **82**, 1068 (2022). https://doi.org/10.1140/epjc/s10052-022-11034-0
95. J.S. Schwinger, Phys. Rev. **125**, 397 (1962). https://doi.org/10.1103/PhysRev.125.397
96. J.S. Schwinger, Phys. Rev. **128**, 2425 (1962). https://doi.org/10.1103/PhysRev.128.2425
97. R. Jackiw, K. Johnson, Phys. Rev. D **8**, 2386 (1973). https://doi.org/10.1103/PhysRevD.8.2386
98. E. Eichten, F. Feinberg, Phys. Rev. D **10**, 3254 (1974). https://doi.org/10.1103/PhysRevD.10.3254
99. A.C. Aguilar, D. Ibanez, V. Mathieu, J. Papavassiliou, Phys. Rev. D **85**, 014018 (2012). https://doi.org/10.1103/PhysRevD.85.014018
100. D. Ibañez, J. Papavassiliou, Phys. Rev. D **87**, 034008 (2013). https://doi.org/10.1103/PhysRevD.87.034008
101. A.C. Aguilar, D. Binosi, C.T. Figueiredo, J. Papavassiliou, Phys. Rev. D **94**, 045002 (2016). https://doi.org/10.1103/PhysRevD.94.045002
102. G. Eichmann, J.M. Pawlowski, J.M. Silva, Phys. Rev. D **104**, 114016 (2021). https://doi.org/10.1103/PhysRevD.104.114016
103. A.C. Aguilar, M.N. Ferreira, J. Papavassiliou, Phys. Rev. D **105**, 014030 (2022). https://doi.org/10.1103/PhysRevD.105.014030
104. A.C. Aguilar, F. De Soto, M.N. Ferreira, J. Papavassiliou, F. Pinto-Gómez, C.D. Roberts, J. Rodríguez-Quintero, arXiv:2211.12594 [hep-ph]